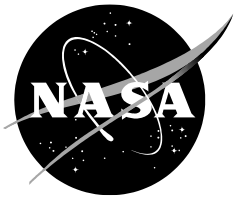
NASA/TM–20260008871



In-Situ Resource Utilization Using Drilling Regolith for Excavation and Analysis of Moon Surface (DREAMS) Hopper for Self-Sustaining Lunar Habitat

** All authors contributed equally to this memo. The names are listed alphabetically by last name.*

Nikita Agrawal
Gretchen Whitney High School, Cerritos, California

Natsumi Aman-Nguyen
Evergreen Valley High School, San Jose, California

Edgar Folmar III
Texas Academy of Math and Science at the University of North Texas, Denton, Texas

Lucianna Ikehara
Cypress High School, Cypress, California

Sam Kowalski
Webb School of Knoxville, Knoxville, Tennessee

Mark Simon
Cypress High School, Cypress, California

September 2026

NASA STI Program Report Series

Since its founding, NASA has been dedicated to the advancement of aeronautics and space science. The NASA scientific and technical information (STI) program plays a key part in helping NASA maintain this important role.

The NASA STI program operates under the auspices of the Agency Chief Information Officer. It collects, organizes, provides for archiving, and disseminates NASA's STI. The NASA STI program provides access to the NTRS Registered and its public interface, the NASA Technical Reports Server, thus providing one of the largest collections of aeronautical and space science STI in the world. Results are published in both non-NASA channels and by NASA in the NASA STI Report Series, which includes the following report types:

- TECHNICAL PUBLICATION. Reports of completed research or a major significant phase of research that present the results of NASA Programs and include extensive data or theoretical analysis. Includes compilations of significant scientific and technical data and information deemed to be of continuing reference value. NASA counterpart of peer-reviewed formal professional papers but has less stringent limitations on manuscript length and extent of graphic presentations.

- TECHNICAL MEMORANDUM. Scientific and technical findings that are preliminary or of specialized interest, e.g., quick release reports, working papers, and bibliographies that contain minimal annotation. Does not contain extensive analysis.

- CONTRACTOR REPORT. Scientific and technical findings by NASA-sponsored contractors and grantees.

- CONFERENCE PUBLICATION. Collected papers from scientific and technical conferences, symposia, seminars, or other meetings sponsored or co-sponsored by NASA.

- SPECIAL PUBLICATION. Scientific, technical, or historical information from NASA programs, projects, and missions, often concerned with subjects having substantial public interest.

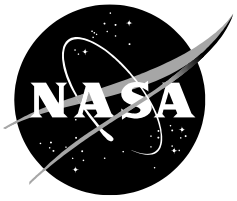
- TECHNICAL TRANSLATION. English-language translations of foreign scientific and technical material pertinent to NASA's mission.

Specialized services also include organizing and publishing research results, distributing specialized research announcements and feeds, providing information desk and personal search support, and enabling data exchange services.

For more information about the NASA STI program, see the following:

- Access the NASA STI program home page at http://www.sti.nasa.gov

NASA/TM–20260008871



In-Situ Resource Utilization Using Drilling Regolith for Excavation and Analysis of Moon Surface (DREAMS) Hopper for Self-Sustaining Lunar Habitat

** All authors contributed equally to this memo. The names are listed alphabetically by last name.*

Nikita Agrawal
Gretchen Whitney High School, Cerritos, California

Natsumi Aman-Nguyen
Evergreen Valley High School, San Jose, California

Edgar Folmar III
Texas Academy of Math and Science at the University of North Texas, Denton, Texas

Lucianna Ikehara
Cypress High School, Cypress, California

Sam Kowalski
Webb School of Knoxville, Knoxville, Tennessee

Mark Simon
Cypress High School, Cypress, California

National Aeronautics and
Space Administration

Ames Research Center
Mountain View, CA

September 2026

The use of trademarks or names of manufacturers in this report is for accurate reporting and does not constitute an official endorsement, either expressed or implied, of such products or manufacturers by the National Aeronautics and Space Administration.

Available from:

NASA STI Program / Mail Stop 050
NASA Langley Research Center
Hampton, VA 23681-2199

Acknowledgments

We would like to thank our mentors, Husni R. Idris and Prachi Panda, for guiding us through the entire process of building this report and concept. They both provided insurmountable understanding and we would not have been able to finish this research project without their support. We would also like to thank Shannon Zelinski and Divya Bhadoria for leading and organizing the Aviation Concept Design Program, along with Jimin Choi, Schelin Ireland, Mikalya Krech, and Micah Borrero for providing us with valuable resources on our research topic. Last but certainly not least, we would like to thank everyone at the NASA Ames Research Center for their hospitality during our in-person visit and for making our experience in this program one of the best.

Table of Contents

ABSTRACT 1

INTRODUCTION 2

BACKGROUND 3

History of Lunar Exploration 3
Challenges During Previous Missions 5

MOTIVATION 5

Challenges of 3D Printing 6
Our Solution 6

CONCEPT OF OPERATIONS 7

Operational Concept Objectives 7
Scope 7
Assumptions and Constraints 7
Operational Concept Scenario 8
Crater Comparison 8
Stage One: Sampling with DREAMS 9
Stage Two: Excavation and Ground Transportation using T-REx 11
Stage Three: Additive Manufacturing 12

SYSTEMS 14

I. DREAMS 14
Drill and Scientific Instruments 14
Specifications 19
Propulsion and Body 20
CAD Rendering 21
Range 21
Energy Budget 26
End of DREAMS Cycle 33
Comparison of DREAMS to Pre-existing Systems 33
II. T-REx 34
Introduction 34
Design Overview 35
Navigation 39
Conclusion 41
III. Lunar Auger Dryer ISRU (LADI) 42
Specifications 43
Connection to LPBF printing 44
IV. Laser Powder Bed Fusion Printing 44
Specifications 45
Impact 46

IMPACT AND CONCLUSION 46

Impact 46
Conclusion 47

FUTURE WORK 48

Making DREAMS Come True 48
The Future of DREAMS 48
SpLASH 49

Refueling Station Launcher *49*
THE HYDRAZINE CHALLENGE 50
T-REX 51
COMMUNICATIONS 52
APPENDIX 53
DERIVATION FOR RANGE EQUATION (SEE EQUATION [1]) 53
REFERENCES 56

Abstract

Over 50 years ago, NASA's Apollo missions answered many of humanity's questions from space to biosciences while advancing computing capabilities. Orbital spacecraft and rovers have transformed our understanding of the moon. Recently, the completion of Artemis II has initiated a new era focused on sustained lunar presence and autonomous exploration. However, a gap remains between scientific resource characterization and technology required for long-term exploration utilizing these resources. For these reasons, we propose a framework comprising of three complementary systems: the Drilling Regolith for Excavation and Analysis of Moon Surface (DREAMS) hopper, the Terrain-adaptive Regolith Excavator (T-REx) rover, and the MoonFall drones. DREAMS identifies and characterizes resource-rich regolith deposits through subsurface drilling and sampling, while T-REx autonomously excavates and transports regolith to a lunar base for further processing. The MoonFall drones aid T-REx with path planning and navigation on the lunar surface. At the base, 3D printers use processed regolith to manufacture components necessary to support sustained surface operations while reducing dependence on earth-supplied materials. Within this framework, these systems provide an operational concept for exploring permanently shadowed regions (PSRs) near the lunar south pole while collecting geological and engineering data through regolith extraction. Through systems engineering analysis, we evaluated the feasibility of integrating drilling, excavation, regolith transport, and additive manufacturing into an in-situ resource utilization (ISRU) architecture while considering the scientific and engineering objectives of this operational concept. Ultimately, Project DREAMS demonstrates an approach to sustainable lunar exploration while simultaneously establishing a foundation for future deep-space human missions.

Introduction

The moon has become the next threshold in a cosmic journey we were always destined for. For almost 70 years, both the National Aeronautics and Space Administration (NASA) and non-NASA organizations have made historic discoveries, answering many of humanity's questions while concurrently inspiring us to dig even deeper. This paper intends to answer the wicked problem "How can in-situ resource utilization create a sustainable living habitat on the moon?" A particular sub-question we explored is "How can aviation-inspired technologies help find a solution to this wicked problem?" As is often the case with wicked problems, there are many answers and it frequently requires multiple methodologies working together. Although the moon has been explored remotely for decades, it is only recently that payloads have been engineered to navigate the terrain via propulsive flight while working in tandem with a rover system towards a greater goal: creating a permanent celestial presence off our blue planet. Our proposal to answer this wicked problem is demonstrated through our operational concept *Project DREAMS*. To further elaborate on the wicked problem, this concept leverages and expands on the effort of the Intuitive Machines 2's Micro-Nova Hopper (μ-Nova "Grace"), NASA's VIPER rover, NASA's IPEx rover, NASA's ERNEST rover, and NASA's MoonFall drone by proposing a system of integrated conceptual spacecrafts to explore the moon from both the surface and the air [1, 2, 3, 4, 5].

The Drilling Regolith for Excavation and Analysis of Moon Surface (DREAMS) hopper is a conceptual machine for an unmanned aerial system (UAS) designed to hop, drill, and examine the lunar surface at an extremely fast pace compared to rovers. The major limitations of rovers are the speed of their operations, their susceptibility to damage, and their ability to collect data over the course of only a few kilometers. This UAS will solve that issue by traveling hundreds of kilometers while also collecting data with degrees of detail not possible by orbiters and efficiency not possible by rovers. The DREAMS hopper will also be able to test the composition of the lunar regolith while investigating its viability of potentially becoming a part of additive manufacturing. A major benefit of our integrated hopper is its ability to support in-situ resource utilization and run tests on the lunar regolith without leaving the sampling site.

From a systems engineering standpoint, the DREAMS hopper is designed to overcome a major operational challenge by combining extraterrestrial flight and rover-like operations into one.

Our operational concept will also use the Terrain-adaptive Regolith Excavator (T-REx) rover. T-REx is a modified version of the Infrastructure Pilot Excavator (IPEx) rover and the ERNEST rover, and it will primarily be used to collect and transport regolith from a chosen excavation site back to Artemis Base Camp (ABC), where advanced 3D printing will occur after a process of refinement and volatile-separation [3, 6]. This rover will follow directions given by the DREAMS hopper to go to the excavation site and extract hundreds of kilograms of regolith that will be then used for future, permanent lunar habitats.

The planned operations may necessitate a path consisting of several kilometers, where the T-REx rover will have to traverse the rugged lunar terrain to reach its targeted destination. To ensure that the path being followed remains viable at all times, MoonFall drones will survey the suggested path to ensure there are no major obstructions that could cause damage to T-REx's systems or hinder traverse.

The final part of our operational concept consists of additive manufacturing through advanced regolith sorting and 3D printing for a future lunar habitat. After the regolith is transported to ABC by T-REx, it will go through a system designed to process the regolith by extracting water and other volatiles [4]. These can be used to make fuel, as a coolant, or for everyday use in the future. Once the regolith is sorted, it will then be powdered and sent to a Laser Powder Bed Fusion (LPBF) 3D printer to make structural components for future, permanent lunar bases that protect against the lunar environment.

Background

This section discusses the history of lunar exploration and challenges during previous missions.

History of Lunar Exploration

When the moon was just starting to be explored in the late 1950s and early 1960s, humans had no idea what was in store for them in the future. Located 384,400 kilometers from Earth, the airless, radiation-scorched Moon remained a dangerous frontier that demanded the invention of entirely new scientific methodologies and tools to reach it.

The birth of the space race and rapid rocket developments of the late 1950s opened the door to lunar exploration. While the Soviet Union led the initial charge toward the Moon, America's competing Pioneer probes suffered a string of early failures [7]. It was not until 1964

that NASA achieved its first major breakthrough with Ranger 7, which successfully transmitted the first close-up images of the moonscape before crashing [7, 8]. Mid-century military breakthroughs and the dawn of the Cold War space race finally brought the Moon within human-reach. The initial phase of lunar exploration relied on flybys and orbiters to map the cratered terrain, paving the way for aggressive surface exploration [7]. During this high-stakes race, both superpowers deployed robotic landers, with the USSR's Luna 9 securing the first soft landing in 1966, before NASA achieved the ultimate milestone of the era by landing the first humans on the Moon during the Apollo 11 mission in 1969 [7]. Following five subsequent Apollo landings and a final Soviet robotic sample return in 1976, dedicated Moon exploration entered a massive, multi-decade hiatus.

The silence was finally broken in 1994 when NASA's Clementine orbiter mapped the entire lunar surface and discovered strong evidence of water ice hidden inside permanently shadowed regions (PSRs) within polar craters [7]. Just a few years later, the Soviet Union's Lunokhod 1 (which had originally introduced robotic driving to the Moon in 1970) found its legacy renewed as a new wave of international space programs looked back toward Earth's satellite. The dawn of the 21st century triggered an expansive lunar renaissance, headlined by orbital mapping fleets deployed by space agencies in Japan, Europe, and India. Concurrently, NASA launched its powerhouse Lunar Reconnaissance Orbiter alongside specialized gravity-mapping probes and kinetic surface impactors [9]. Far outlasting their baseline mission timelines, these assets compiled a massive amount of data detailing the Moon's rugged topography, radiation environment, and structural composition [9].

Today, the Moon has evolved into a highly competitive international spotlight, defined by China's historic far-side Chang'e touchdowns and robotic sample retrievals, India's milestone Chandrayaan-3 landing at the lunar south pole, and the ongoing operations of NASA's crewed Artemis campaign [10, 11]. As of 2026, NASA remains the premier leader in lunar operations, having successfully launched four astronauts around the Moon aboard Artemis II to pave the way for a permanent human return [11]. Alongside these human milestones, NASA's veteran Lunar Reconnaissance Orbiter (LRO) continues to gather critical surface data, while the agency's Commercial Lunar Payload Services (CLPS) program drives a steady pipeline of American robotic landers to the surface such as legacy mission Intuitive Machines 2 (IM-2) [12]. Looking toward 2028 and beyond, NASA, in collaboration with international partners like JAXA and ESA and utilizing CLPS, is actively designing sustainable infrastructure, deep-space habitats,

and autonomous surface vehicles [10, 12]. These public-private initiatives are laying the groundwork for a highly collaborative era, leaving the door wide open for next-generation concepts such as ours to shape the future of humanity's expansion across the cosmos.

Challenges During Previous Missions

Our operational concept utilizes a system that did not fulfill its mission goal. However, this is not uncommon; if success is defined by a mission that completely met all primary mission objectives, then only seventy-one of one hundred and forty-three (71/143) global robotic missions to the Moon have achieved total success [13]. By analyzing these challenges, we hope to develop resolutions to them that would ensure 100% success and prevent our concept, along with future ones, from encountering comparable outcomes.

Specifically, one of the aviation systems (DREAMS hopper) of our operational concept resembles the following mission's system: IM-2's Micro-Nova Hopper (μ-Nova "Grace"). During the IM-2 mission, the primary challenge was an off-nominal host vehicle (Nova-C "Athena" lander) orientation that mechanically constrained and prevented the deployment of the μ-Nova hopper [1]. However, for the purpose of this project, we will assume a normal landing for the large lander.

Motivation

There has been a substantial increase of interest in lunar exploration over the past few years. But traveling between the Moon and the Earth takes a lot of resources such as transportation of materials, devices, fuel, and logistical planning. Therefore, a race has begun to have a permanent human presence on the Moon (see Figure 1). This has fueled the idea of building a safe, viable human habitat on our closest celestial neighbor.

The overarching motivation for Project DREAMS came from this necessity to establish a home base for the astronauts and researchers on the Moon for future exploration of the lunar surface as well as other planetary bodies. In this project, we explored and researched the idea of using lunar regolith to build infrastructure, buildings, labs, and dwellings using 3D printing methods.



Figure 1. NASA's vision of the Moon Base [26]

Challenges of 3D Printing

As with any innovation, using regolith for 3D printing came with its own challenges. To minimize the dependence on Earth-supplied materials and use of polymers and additives, we found a self-sustaining method of 3D printing called Laser Powder Bed Fusion (LPBF) [14]. The optimal composition for this process is mafic and basalt rich regolith. Since the Moon is highly unexplored and the properties of lunar regolith are somewhat unknown, a deep study and analysis of different craters and regolith composition was performed. The next challenge was to procure and transport lunar regolith from the chosen crater site to the moon base for 3D printing since the distance between the sites ranged from a few kilometers to thousands of kilometers. Due to the irregular and uneven terrain on the Moon, this created a big challenge.

Our Solution

We propose an aviation-based system, inspired by drones on earth, which is able to cover long distances in a short time while also being able to overcome terrain-related constraints of the lunar surface.

Concept of Operations

The concept of operations will address the scope and details of our in-situ resource utilization using the DREAMS hopper for a self-sustaining lunar habitat operational concept.

Operational Concept Objectives

The objective of this operational concept is to analyze regolith and determine if certain areas of the lunar surface are suitable for 3D printing. Once a suitable excavation site is determined, the regolith will be collected, transported, sorted, and fed into a printer that will use LPBF to create usable material. With this material, large-scale manufacturing of structures (like walls and bricks), maintenance tools, and replacement parts will be possible, allowing for the creation of a sustainable living habitat.

Scope

For the scope of this project, everything is explained in a "day of operations" style. Therefore, throughout this paper, operations are described as if one of each type of device (one DREAMS hopper, one T-REx rover, and one MoonFall drone) is being used. In the case of the actual implementation of our operational concept, we suggest implementing multiple T-REx rovers, due to the rover's slow nominal speed relative to DREAMS and 3D printing demands.

Please also note that the lack of public and detailed information about the moon geology and the state of the art of technologies led the team to make simplifying assumptions and engineering guesses that may have resulted in inaccuracies in the assessments and conclusions made. The concept and associated assessments are preliminary, and more thorough analysis is needed based on more accurate information when available.

Assumptions and Constraints

The concept of operations is based on a day in the 2030s, with the assumptions that there have been multiple visits to the moon and there is an established Moon base or lab (Artemis Base Camp, or ABC) for humans along with a communication system, both between humans and lunar machines (including hoppers and rovers). Furthermore, optimal weather conditions are assumed on the moon implying there are no electrostatic or dust storms to inhibit the functionality of equipment. It is also assumed that all systems integrate smoothly and the concept of operations does not reflect any anomalies (e.g., the malfunction of the O3D LiDAR landing

system). In addition, it will be assumed that the hopper and rover can be constructed without any material, cost, or administrative constraints. The timeline of the project is discussed but the cost and feasibility analysis is beyond the scope of this paper.

Operational Concept Scenario

The day of operations will identify the specifications and planning of Project DREAMS and provide details to bridge the gap of what each system is designed to do.

Crater Comparison

Before the day of operations, it is important to select a landing site and an excavation site. Three craters were shortlisted: Shackleton, Amundsen, and Aitken.

They were compared in Table 1 using four main criteria - radiation, safety for humans, regolith composition, and vicinity to home base. These factors were taken into consideration to ensure the safety of astronauts and equipment while procuring basalt-rich regolith which is optimal for 3D printing as well as keeping in mind the logistics for traveling between the home base and regolith collection sites.

Table 1. Crater Comparison

Name	Shackleton Crater	Amundsen Crater	Aitken Crater
Radiation	✅ low	🟥 high	🟥 high
Safety for Humans	✅ yes	🟨 somewhat	🟥 no
Composition	🟥 felsic, dominated by anorthosite and noritic crust	🟨 mostly felsic, contains mafic and iron-rich materials	✅ mafic (basalt-rich)
Vicinity to Shackleton	-	✅ 152 km	🟥 2200 km

As shown in Table 1, Shackleton regolith is entirely felsic (high in silica content and low in iron content) and unsuitable for 3D printing. Like Shackleton, Amundsen is mostly felsic but contains some iron-rich parts which may be suitable for 3D printing. However, Aitken is mafic (low in silica content and rich in magnesium and iron) *and* basalt-rich, which makes it the most optimal in terms of composition since it can be used for our LPBF 3D printing method.

Additionally, while the distance from the home base to Shackleton is negligible, the other craters are farther away as seen in Table 1. This creates a tough challenge in our wicked problem since it will be considerably harder to cover these long distances via ground transportation, such as rovers.

Overall, the following conclusions were made from this crater comparison. Shackleton is the best crater for establishing the moon base where humans will live. Past and future NASA missions plan to land in this crater as well due to its partially illuminated and partially shadowed regions. Amundsen is the closest to Shackleton home base, making it the most practical for excavation given that the DREAMS hopper and T-REx rover have limited range, but it does not have the ideal composition. Aitken is the only crater with optimal composition, but it is extremely far from Shackleton. Therefore, the choice of excavation crater is up to user discretion; however, we will cover mainly the Shackleton and Amundsen cases in this paper as they currently seem most practical.

Stage One: Sampling with DREAMS

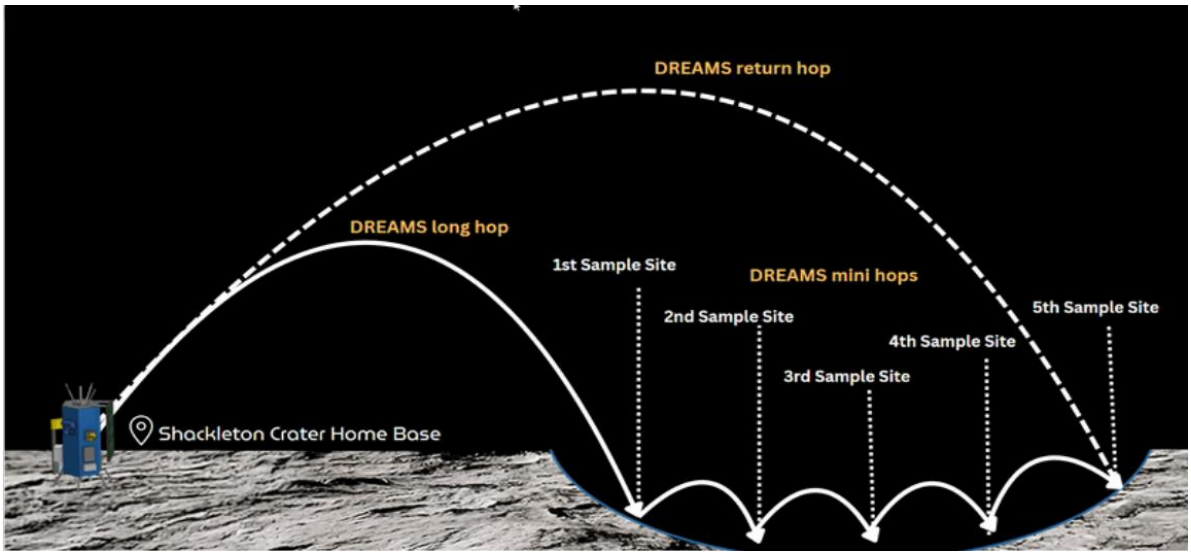


Figure 2. Proposed flight plan for DREAMS Hopper

Due to the long distances between home base and two of the proposed excavation sites, there is a problem of transportation. There have been moon hoppers designed in the past to hop around and explore, and rovers that can traverse the lunar surface. However, there is no composite system that can solve our wicked problem. This is where the first aviation component and our innovation come in–the DREAMS hopper.

As shown in Figure 2, DREAMS is meant to do one outbound long hop, four mini hops, and one inbound return hop between the home base and exploration site. The outbound hop is meant to get the hopper from its initial landing site to the first regolith sampling site. Each mini hop is meant to land at a new sampling site within the chosen crater. The return hop takes the hopper back to the landing site and home base from the fifth and final sampling site.

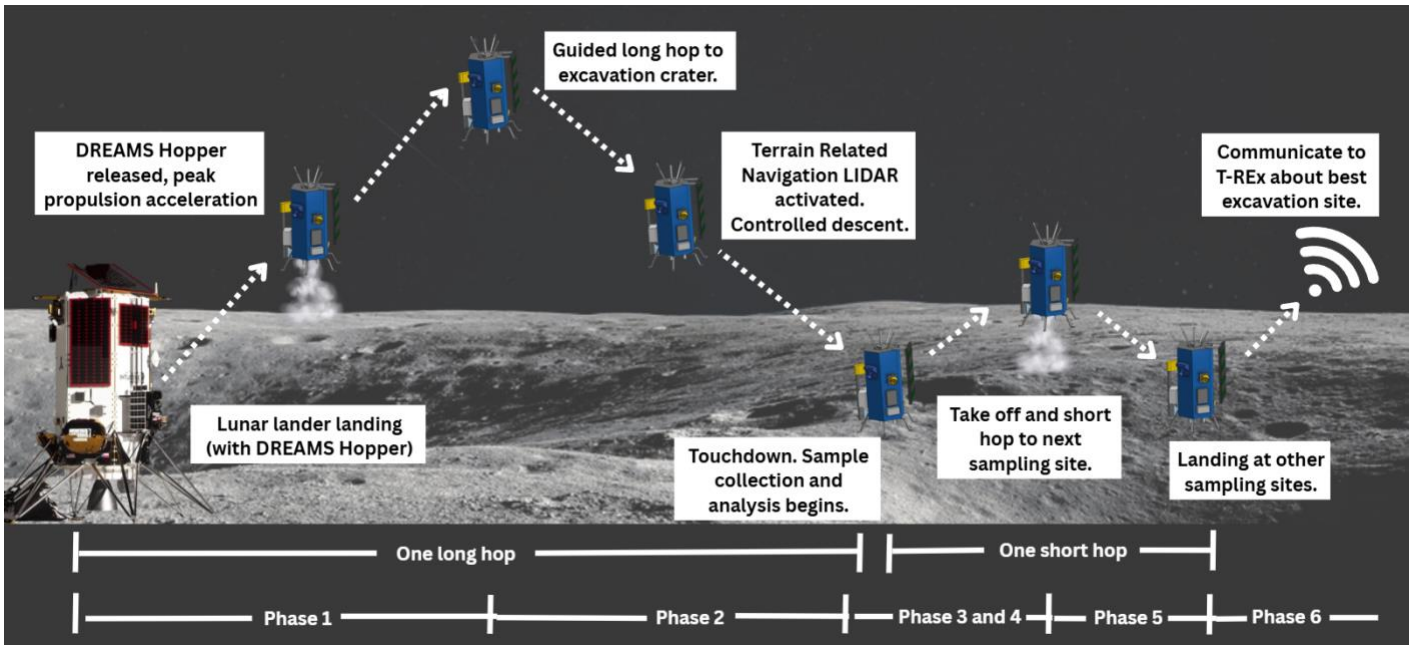


Figure 3. Detailed overview of one outbound hop and one mini hop of the DREAMS hopper

DREAMS's "day" of operation begins from the touchdown of the lunar lander and ends at the point where DREAMS has returned and enters preparation for the next cycle. DREAMS will follow and repeat a seven-phase cycle, which will proceed as follows and is shown in Figure 3:

Phase 1: Transit to excavation crater or PSR

This includes the landing of the lunar lander with the DREAMS hopper, the release of DREAMS from the lander, and a guided long hop to the excavation crater.

Phase 2: Descent and Landing

This entails using Ocellus 3D LiDAR (in our paper, it will be abbreviated as O3D LiDAR) for autonomous landing site selection to ensure a controlled and safe landing.

Phase 3: Regolith Survey

Once the hopper touches down, the spectrometers are activated to survey the regolith.

Phase 4: Conditional Drilling and Analysis

At the first landing site on the excavation crater (also the first sampling site), the drill brings up a sample. On-site analysis determines properties like temperature, composition, and radiation.

Phase 5: Mini Hopping

Sample 1 collection complete. Mini hop to the second of five total sampling sites. Total of 4 mini hops.

Phase 6: Communication to T-REx and Return

After visiting five sample sites, DREAMS communicates to the T-REx rover about the best excavation site of the five sites it just visited. Then, it begins its return long hop to home base with all 5 samples it collected.

Phase 7: Refuel/Recharge

At home base, the hopper drops samples at the lab. It will refuel and recharge as needed before leaving to visit more sampling sites.

These phases will be explored further later in this paper. It is important here to note the range (see *Range* section under *DREAMS*) of the DREAMS hopper, as this significantly impacts prior infrastructural investment and overall feasibility. The one-way range of the DREAMS hopper is 75 kilometers, and in a standard drilling cycle, the hopper can travel to a maximum of 15 kilometers out and back from its refueling location.

<u>Stage Two: Excavation and Ground Transportation using T-REx</u>

The T-REx rover is another one of our innovations, but for ground transportation. It gets its name from its ability to intelligently navigate lunar terrain as well as quickly excavate and transport regolith between the chosen site and home base, like a smart, hungry T-Rex dinosaur.

The phases of the T-REx rover are depicted in

Figure 4. When T-REx reads the signal sent by DREAMS, an empty T-REx departs from the home base to the site communicated by DREAMS. It is guided by the MoonFall drones,

which provide constant surveillance data. This data allows for safe path planning and helps avoid any terrain-related obstacles en route to the proposed excavation site and back. Two systems will be used to aid the path planning process: the Systems Health Enabled Real-time Planning Advisor (SHERPA) and the Exploration Ground Data Systems (xGDS) in order to effectively and safely create a route for T-REx to follow [15, 16]. At the excavation site, the bucket drums on T-REx are lowered to excavate the regolith. Once full, T-REx begins its return journey to the moon base, where regolith will be sorted and 3D printing will occur.

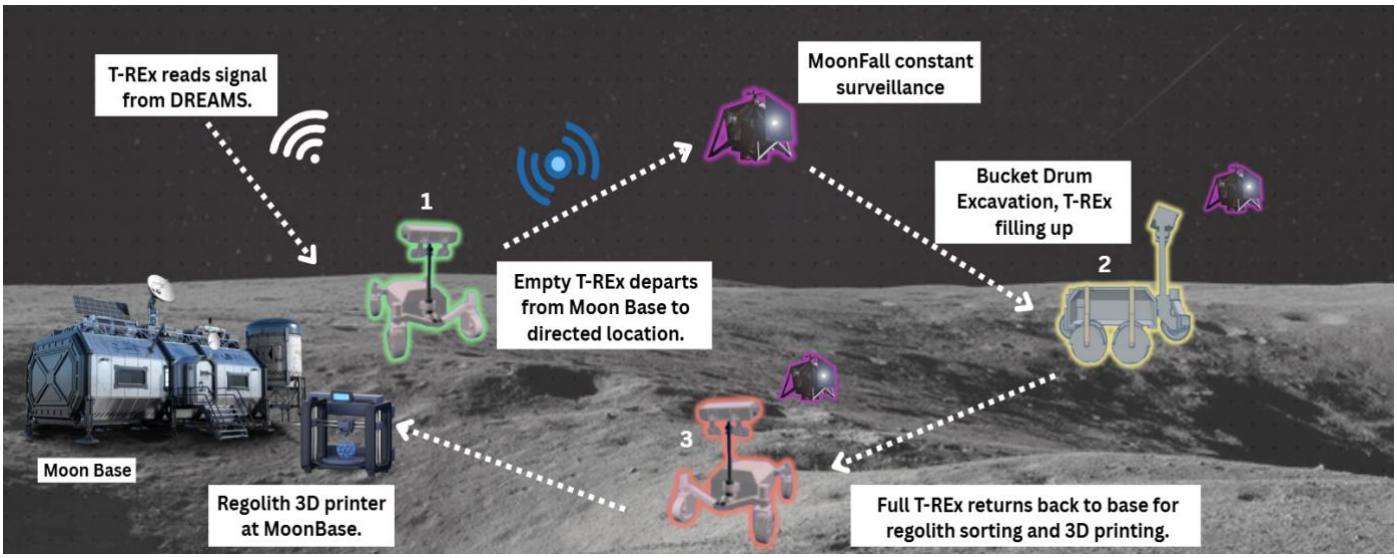


Figure 4. Detailed overview of the path and tasks of T-REx rover and MoonFall drone (shown in purple)

Stage Three: Additive Manufacturing

Additive manufacturing converts the lunar regolith excavated by T-REx into constructed components that can be used around the home base. Once the excavated regolith is sent back to the home base, the material is put through a series of systems that support volatile extraction and 3D printing.

The excavated regolith first makes its way to the Lunar Auger Dryer ISRU (LADI), where water can be separated from the regolith in order to extract volatiles. The material passes through an inlet hopper, where oversized particles are filtered out to avoid damaging the system [17]. Once filtered, the remaining regolith passes through the heated auger casing. As regolith passes through the auger, ice content from the regolith sublimates into water vapor, which is then

collected by a cold trap [17]. Any water vapor collected can be transferred to separate systems for volatile extraction. The remaining dried regolith then exits the system.

Before the dried regolith enters the 3D printer, it must be crushed and powdered. LPBF 3D printing requires that the feedstock can be spread into thin, even layers [14]. This helps to reduce the chances of defective parts and inconsistencies within our system.

After the regolith is powdered, it is given to the LPBF printer. The printer spreads the regolith powder across the build plate and uses a laser to fuse specific areas according to a 3D

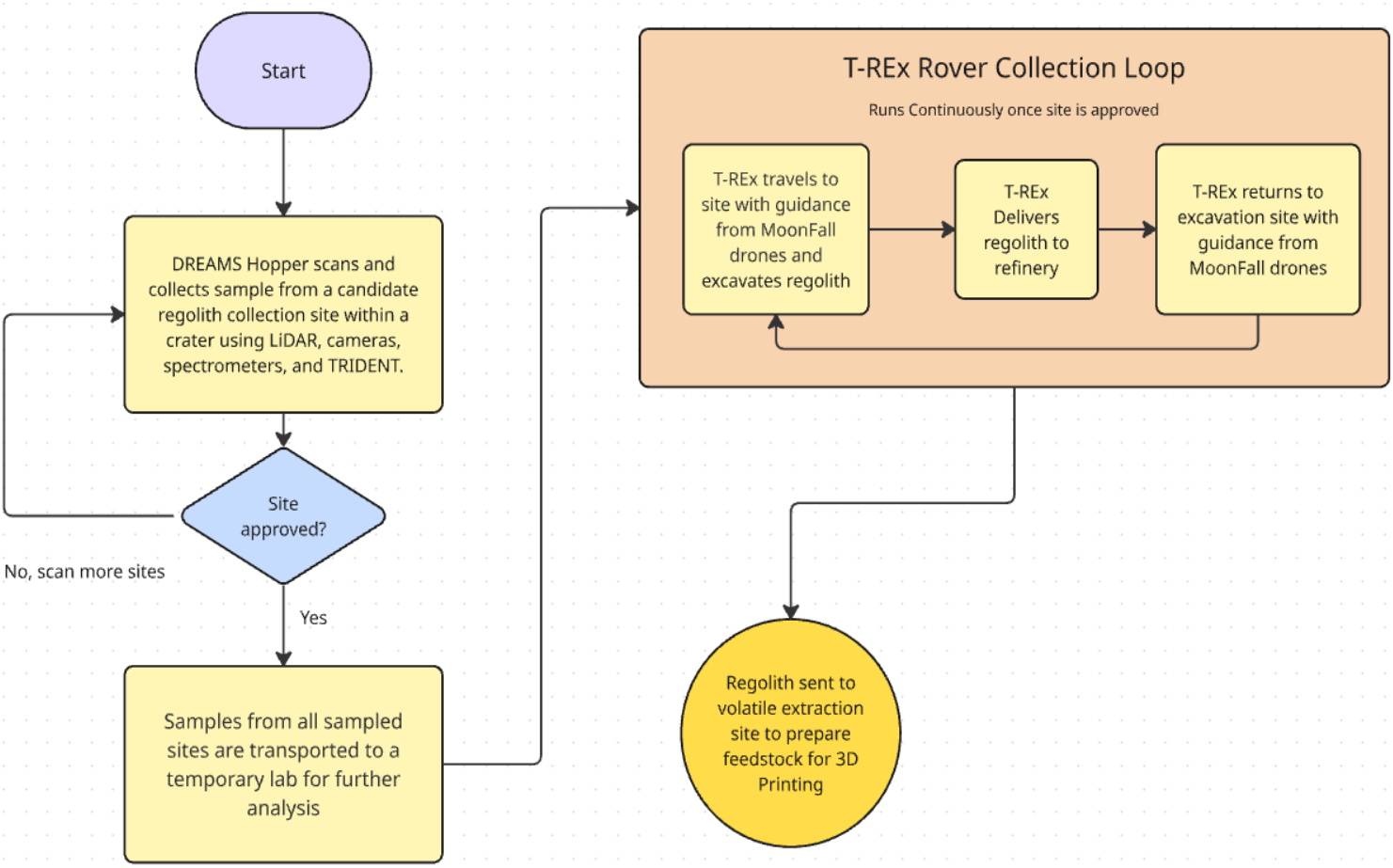


Figure 5. Various steps in the operational concept scenario

model [14]. With LPBF, we intend to build numerous components that can be used around the home base. These printed pieces include, but are not limited to, bricks, shielding tiles, sample trays, equipment mounts and replacement parts. Protective components that are printed can be arranged around a pressurized living module to provide protection.

Figure 5 summarizes the three stages described above in the form of a flowchart. This flowchart represents the various steps in the operational concept scenario. The flowchart's

"Start" point assumes that the lunar lander had no issues landing and that the DREAMS hopper was able to reach the excavating crater.

Systems

I. DREAMS

To test the regolith for composition and viability, our concept requires a moon hopper that has a drilling system and multiple testing devices. From a systems engineering perspective, it would also need to have a long range (≥30 km) and be able to land in many different locations.

To fit these criteria, we propose the DREAMS (Drilling Regolith for Excavation and Analysis of Moon Surface) hopper. This hopper consists of spectrometers, a drill, cameras, radiometer, and LiDAR, which are used to access different areas of the lunar surface and analyze the regolith in a variety of ways, along with special propulsion engines that maximize fuel efficiency and hopping range.

Drill and Scientific Instruments

To determine if the lunar regolith from a certain area is suitable for 3D printing, we must test to figure out its composition (including metals, volatiles, and even water), temperature, and particle size and roughness. To do this, we have selected certain parts of NASA's VIPER Rover (NSS, TRIDENT drill, NIRVSS, MSolo) and Intuitive Machine's Micro-Nova Hopper (LRAD, wide angle camera, narrow angle camera, landing legs, propulsion system). The functionality of each instrument is listed below, along with some proposed modifications to fit everything on the DREAMS hopper.

LRAD: Lunar Radiometer (from Micro-Nova hopper)

LRAD, or Lunar Radiometer, (shown in Figure 6) is a light device equipped with thermopile sensors to accurately collect data on the temperature and roughness of the lunar surface and the radiation around it. LRAD is able to look at surface roughness [18], which includes packing density, size distribution, and complex geometry of individual regolith grains and rocks [19]. It can also determine surface brightness temperature [18], which can help tell the thickness of the soil layer [20] and detect the presence of buried materials like water, titanium, and iron. LRAD will be used to determine whether a potential excavation site is safe for equipment, and whether that site is safe for humans should a base ever be set up there.

Wide angle (144º x 104° FOV) camera (from Micro-Nova hopper)

Another device featured on the μ-Nova hopper, the wide angle camera (shown in Figure 6), inspects the section of lunar surface with which DREAMS is about to make contact [1]. It is aimed at 45° off-nadir, or from the ground, and provides broad situational awareness and context for the local terrain [21]. This will help ensure DREAMS does not land on terrain that may damage it.

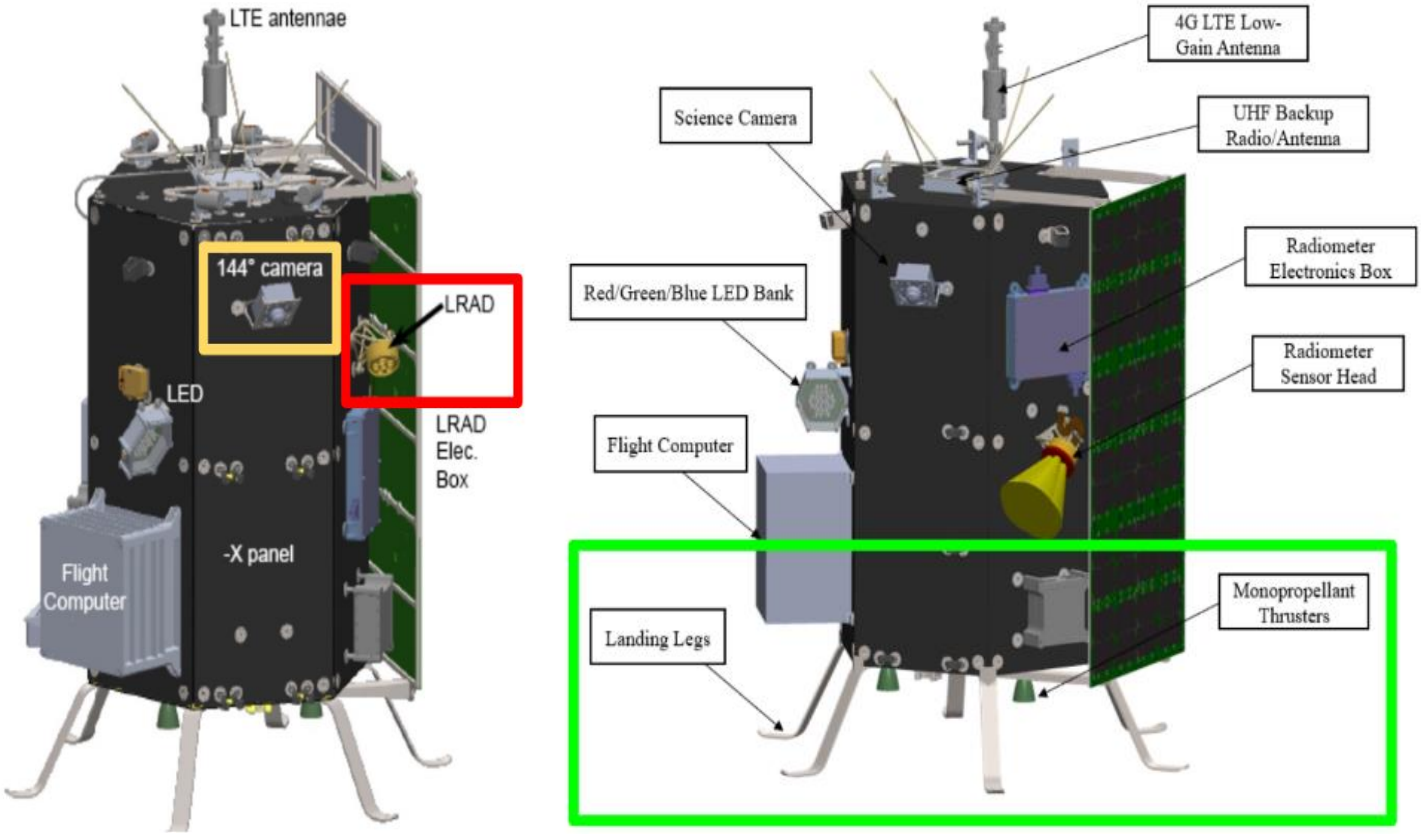


Figure 6. Micro-Nova hopper [21] highlighting LRAD, wide angle camera, landing legs, and thrusters. Narrow angle camera not pictured.

Medium/Narrow angle (51° x 39° FOV) camera (from Micro-Nova hopper)

The narrow angle camera serves a similar overall purpose as the wide-angle camera. This camera is pointed nadir. It oversees high-resolution scientific mapping, can generate digital terrain models, and resolves surface details [21]. The pictures it takes will add more detail to the current mapping of the lunar surface.

NSS: Neutron Spectrometer System (from VIPER rover)

The NSS (see Figure 7) works by detecting the changes in energy and number of small particles called neutrons. Neutrons are constantly emitted by the lunar surface and the NSS is able to search for them up to three feet below the surface. It was originally developed to search for water, since neutrons have a significant drop in energy when they come into contact with another atom of similar size (such as a hydrogen atom). When this energy drop is detected by NSS, it could mean that hydrogen or another similar volatile is present. Although the primary goal of DREAMS is not to identify water, hydrogen-rich sections of the lunar surface are useful, as hydrogen can be separated and used to make a variety of other compounds. One of these compounds could be hydrazine, which fuels DREAMS and has the chemical formula N_2H_4.

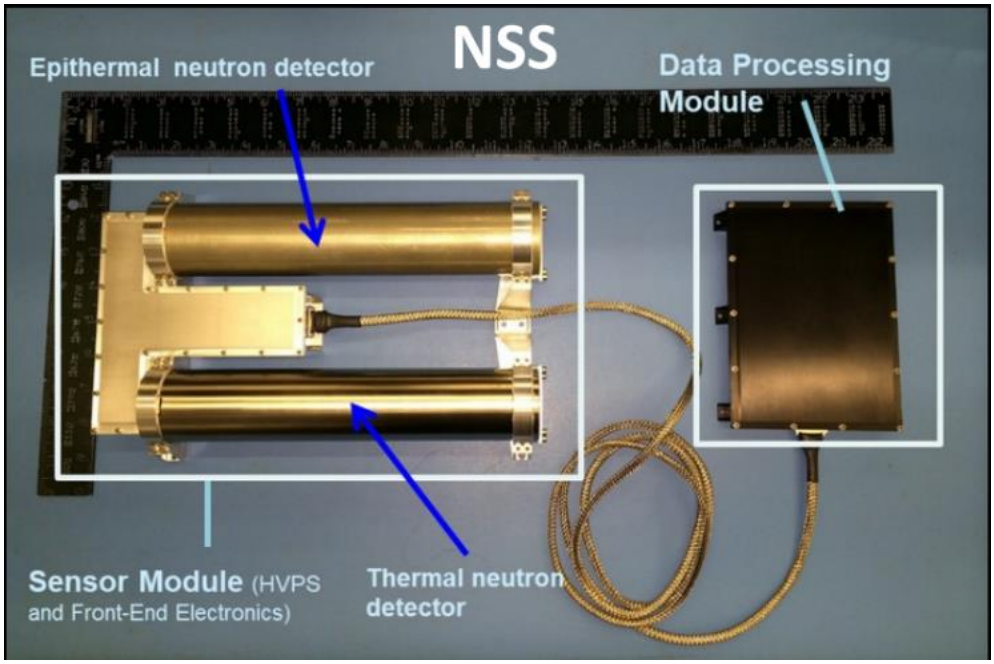


Figure 7. Neutron Spectrometer System [27]

TRIDENT: The Regolith and Ice Drill for Exploring New Terrains (from VIPER rover)

TRIDENT is a 3.28-foot (1 meter) drill designed to dig into the lunar surface. Once hydrogen is detected by the NSS and LRAD deems the site suitable, DREAMS will begin to drill.

TRIDENT is a rotary percussive drill, which means it spins to cut into the ground while hammering to break up hard material, making the drilling process more energy efficient. The tip of the drill has carbide cutting teeth that are harder than steel and can maintain their sharpness.

The drill tip also contains a temperature sensor that takes readings below the surface. The drill string is lined with flutes, which transport drill cuttings up to the surface as TRIDENT spins. Meanwhile, the rotating brush sweeps soil off the drill and into a chute, forming a neat pile on the ground. TRIDENT works by bringing 10 cm bites of regolith to the surface. The spectrometers quickly analyze the sample before volatiles dissipate in transportation before the drill goes back down for another bite. Each bite is piled on top of the other to form a pile. The individual parts of the drill explained above can be seen in Figure 8.

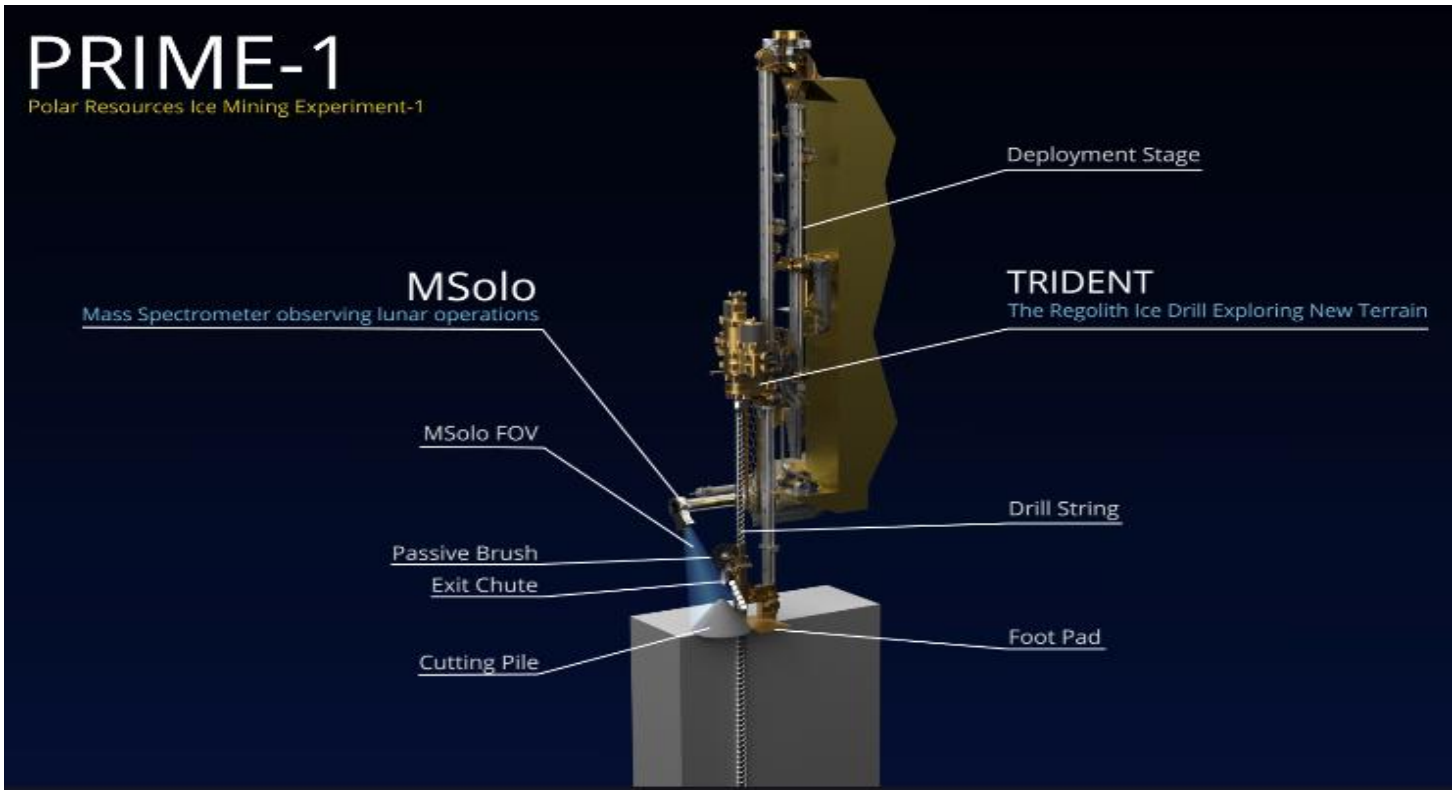


Figure 8. PRIME-1 system, including the TRIDENT drill and MSolo spectrometer [28]. Note: that MSolo will likely not be attached to TRIDENT as shown in this figure on the DREAMS hopper

For the DREAMS hopper specifically, the drill will be modified from 1 meter tall to 0.5 meter instead. This is because the hopper itself is 1.2 meters tall, so having such a large drill would be too bulky and adds too much mass. This contributes to a significant weight decrease in TRIDENT. The only drawback to this would be that the drill will only be able to dig 0.5 meters below the surface, but this depth should be sufficient for the purposes of Project DREAMS.

NIRVSS: Near-Infrared Volatiles Spectrometer System (from VIPER rover)

After NSS detects the presence of hydrogen, NIRVSS (see Figure 9) detects the source of these hydrogen atoms, whether it is pure hydrogen, hydroxyl, or bonded with oxygen to form water. The spectrometer also uses light and optics to determine presence of certain minerals and ices, including but not limited to frozen carbon dioxide, ammonia, and methane [22]. There are two other tools attached to NIRVSS. The Spectrometer Context Imager is a broad-spectrum camera that creates seven-color images to analyze the composition of regolith in fine resolution. Specifically, it can determine the soil's mineralogy, regolith maturity based on space weathering, and geotechnical properties like texture, grain size, and 3D structure. The Longwave Calibration Sensor measures surface temperature and can determine things like porosity based on the regolith's thermal inertia [22, 23].

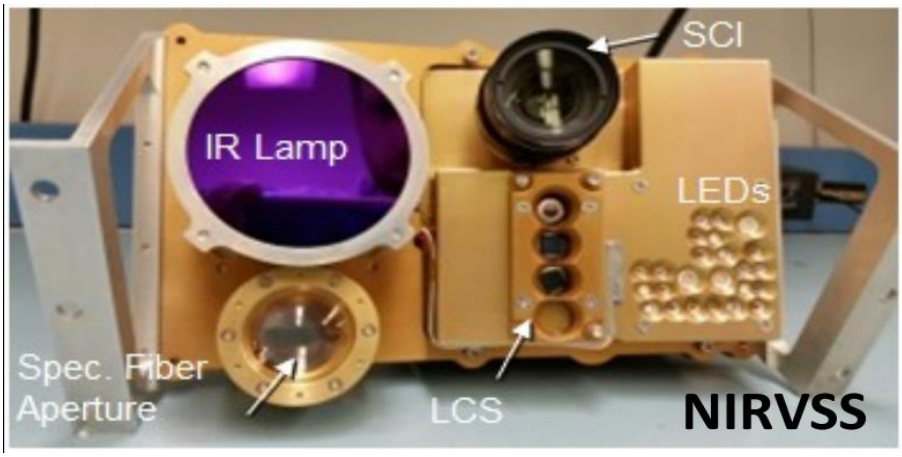


Figure 9. Near-Infrared Volatiles Spectrometer System [27]

MSolo: Mass Spectrometer Observing Lunar Operations (from VIPER rover)

The MSolo (see Figure 10) identifies low-weight volatiles from 1-100 amu, such as carbon monoxide, water vapor, and oxygen [23]. It is usually activated after touchdown to understand which gases are lunar-based, and which are introduced from the hopper or lander [22].

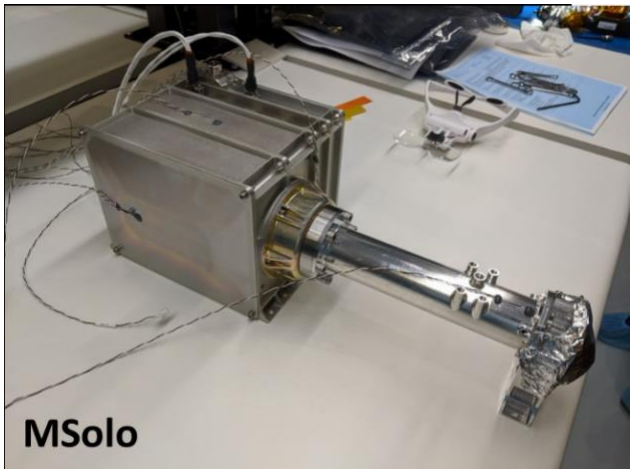


Figure 10. Mass Spectrometer Observing Lunar Operations [27]

Ocellus 3D LiDAR

The DREAMS hopper mitigates the risk of tipping over during landing by integrating the NASA Goddard Space Flight Center's Ocellus 3D LiDAR system (O3D LiDAR). The O3D LiDAR system is a compact, low-power active sensor that utilizes near-infrared lasers and a fast-scanning micro-electromechanical system (MEMS) mirror to create centimeter-scale 3D elevation maps onboard the craft [24]. Operating under the engineering baseline (set forth by IM-2's unfortunate failure) that passive optical navigation is insufficient in dark polar terrain, our proposed architecture will leverage the Ocellus system's dual-mode capability [24]. It functions as a long-range altimeter at an altitude of ~2 km, then automatically transitions into a high-resolution hazard detection mode below 200 meters [24]. As it generates its own light source to bypass the extreme surface shadows, this system provides a lighting-independent terrain profile to secure stable host-vehicle (now Nova-C "Athena" lander or DREAMS hopper) placement on any day of operations [24].

Specifications

The DREAMS hopper will be 1.2 meters in height and 0.4 meters in diameter and will weigh approximately 88 kilograms. DREAMS will be 20% taller than the μ-Nova hopper [1]; this is to account for the extra systems needed, including the TRIDENT system. μ-Nova weighs 39 kgs [1]; in comparison, DREAMS will weigh 88 kgs due to the added systems and extra fuel.

Propulsion and Body

Monopropellant hydrazine engines

DREAMS will have four 150 N monopropellant hydrazine engines. According to data from the Ariane Group, hydrazine engines tend to have a thrust range of 40-110% their listed thrust [25]. Thus, a 150 N hydrazine thruster could provide thrust from ~60-165 N. At maximum thrust during takeoff (assuming 150 N per engine even though the theoretical maximum of the engines is likely 165 N), DREAMS will have a thrust-to-weight ratio of 4.20 (150 N per engine × 4 engines / (88 kg 1.622 m/s^2) = 4.20). Additionally, interpolating data from 20 N and 400 N monopropellant engines, the DREAMS thrusters will have a mass flow rate of 0.45 g/s per Newton of thrust (~27-74 g/s flow rate depending on the thrust) [25]. The total fuel capacity onboard will be 23 liters, with 20 for intended usage every trip and 3 for reserve fuel. DREAMS has a 20-liter fuel capacity because it provides the necessary range, which will be further described later in this paper, and is not large enough that the fuel tanks take up too much space of the hopper. DREAMS will likely have some smaller hydrazine engines used for attitude control, but the amount of hydrazine used for these is very small and negligible for our range calculations.

CAD Rendering

To understand how all the systems would fit onto the DREAMS model, we created a simple CAD rendering of DREAMS and its systems. Figure 11 shows DREAMS from multiple angles and labels its
subsystems.

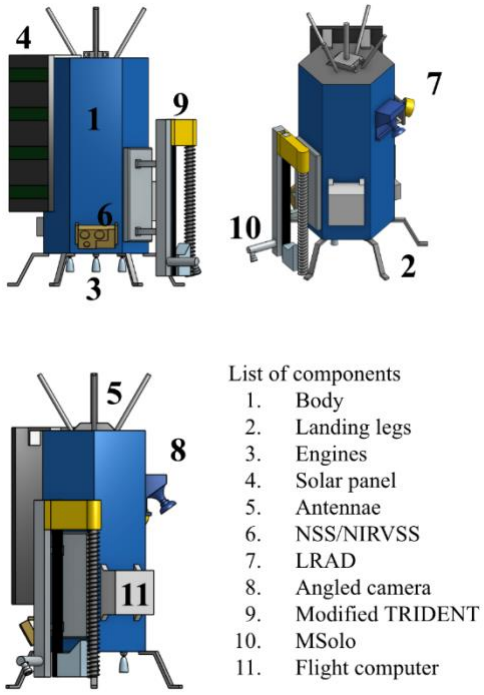


Figure 11. CAD rendering of DREAMS

Range

The range for DREAMS varies depending on what its goal is. The Micro-Nova hopper has a range of 25 km with a 10 kg payload [1]. Given the dimensions and range of the Micro-Nova hopper, we estimated the fuel capacity of Micro-Nova to be ~5.5-6 liters. Let the range function for μ-Nova be defined as r(L, F, I_{sp}, m), with the four variables defined as shown in

Table 2.

Table 2. Default Values of Variables

Variable	Definition	Fixed Value
L	Liters of fuel used on takeoff for a specific trip	8 L
F	Thrust force provided by engines	600 N
I_{sp}	Specific impulse (fuel efficiency) of engines	220 s
m	Mass of hopper	88 kg

For our long hops, we assume a 45-degree ballistic hop where the hopper uses 80% of its planned fuel on takeoff and 20% on landing. Additionally, we assume constant mass for the duration of the hop. The mass of DREAMS could be made variable using Tsiolkovsky's rocket equation, but for simplicity, we assume the mass of DREAMS is constant and equal to DREAMS' wet mass at takeoff. Both of these assumptions make our range estimate conservative. Furthermore, we believe our range estimate to be fairly accurate as the propellant only accounts for a maximum of 25% of the mass of DREAMS and an optimized-pitch trajectory does not substantially increase range given the same amount of fuel. We used the specific impulse equation $I_{sp} = F / (\dot{m} \times 9.81)$ where $\dot{m}$ is the mass flow of hydrazine. Substituting this to find the time of initial launch and then substituting in kinematics equations, we find that r(L, F, I_{sp}, m) simplifies to equation (1):

$$r = \frac{\left(9.81 I_{sp}\right)^2 (1.021L)^2}{1000}\left(\frac{\sqrt{2}}{4mF} + \frac{\sqrt{2}}{3.244m}\left(\frac{\sqrt{2} + \sqrt{2 - \frac{3.444\sqrt{2}m}{F}}}{2m} - \frac{1.622}{F}\right)\right) \quad [1]$$

The division by 1000 is simply conversion from meters to kilometers. Figure 12 shows a graph of r(F), which shows that the more engine force we have, the farther the hopper's range will be. However, there are diminishing returns as the more powerful the engines get, the quicker they burn through the fuel; indeed, the graph approaches an asymptote in equation (2).

$$r = \frac{(9.81 I_{sp})^2 (1.021L)^2}{1000 \times 1.622m^2} \quad [2]$$

In Figure 12, a total of 600 Newtons of engine force results in a 20.4 km range and an infinitely powerful engine would yield a range of 24.7 km. However, equation (2) does not account for the size and mass of the hydrazine engines; the weight of larger engines negatively impacts the range of the hopper. To balance these conditions, we decided on a total of 600 Newtons of force from the engines, spread out across four 150 N engines.

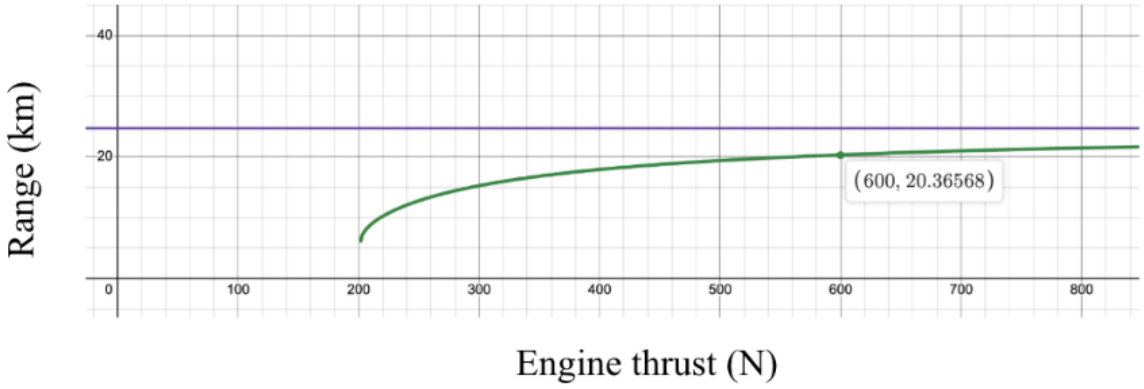


Figure 12. r(F) with I_{sp} = 220, m = 88 kg, and L = 8

Another insight we can discover from this equation (2) is that increasing fuel quadratically increases range. Because of this, doubling the fuel quadruples the ballistic range of that hop. This leads to an important point: minimizing hops using the same volume of fuel will always increase range, so it is better to do as few hops as possible. Thus, DREAMS will only land to refuel or drill. Figure 13 shows the comparison of fuel and range. As seen in Figure 13, a hop that uses 16 L on takeoff travels 81.5 kilometers, while two 8 L hops only travel 40 kilometers.

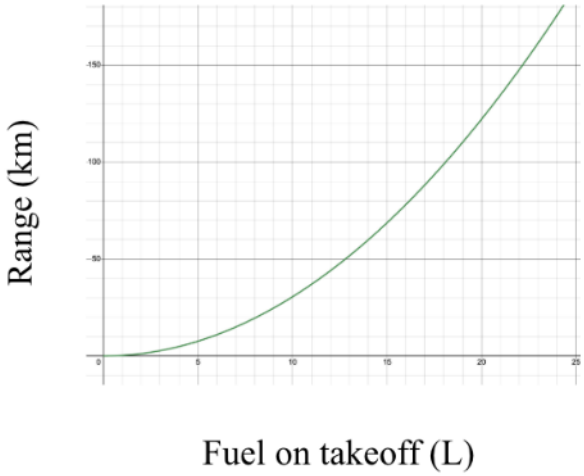


Figure 13. r(L) *with I_{sp} = 220, m = 88 kg, and F = 600 N. r(8) = 20.3, r(16) = 81.5.*

This connection has range implications. The range of a hop that uses 20 liters total, meaning 16 on takeoff and 4 on landing, is 81.5 km. We will assume the maximum range of this hopper, however, is 75 km. The reason for this is a ballistic hop of this size will result in extreme landing speeds that 4 liters of fuel will likely not be able to stop, so we will assume a lower percentage of fuel used on takeoff. In reality, the flight trajectory for this big hop will likely not be completely ballistic but rather involve a gradual pitch change on takeoff. However, the range of a hop that burns 8 liters of fuel on takeoff can only travel 20 km. When we add in the mini hops necessary for drilling, this range decreases to about 15 km, as we will shortly explain.

Standard Drilling Cycle

There will be three types of hops for a standard drilling phase: the outbound hop, the mini hops, and the return hop. We will demonstrate a standard cycle where the desired drilling location is a maximum of 15 km from a refueling station. For a cycle where the drilling spot is not as far away, the hopper will consume less fuel. Below, Table 3 shows the fuel consumption of a full 15 km trip with four 250-meter mini hops in between. This consumes 19.66 liters of fuel, which is within the 20-liter fuel capacity. Though, this trip will likely take less fuel for a number of reasons. Improvements on our model will yield this difference; the flight trajectory can be further optimized, meaning each hop will require less fuel for the same distance, and the change in mass can be modeled using Tsiolkovsky's rocket equation instead of keeping the mass constant at wet mass, providing a less conservative approximation of range. The trajectory is not the only thing about the flight that can be cleverly changed; the mini hops can be organized strategically so that one of the mini hops is shorter than 250 m or the return hop is less than 15 km. Even if a trip ends up consuming more than 20 liters of fuel for whatever reason, we can dip into the 3 liters of reserve fuel on the final landing.

Table 3. Fuel consumption of standard drilling cycle for DREAMS. The total fuel consumption is 19.66 liters

Hop Type	DREAMS mass (beginning, in kg)	Distance required (km)	Fuel required (liters)	Fuel remaining (liters)	DREAMS mass (end, in kg)
Outbound hop	88	15	8.57	11.43	79.26
Mini hop 1	79.26	0.25	0.98	10.45	78.26
Mini hop 2	78.26	0.25	0.97	9.48	77.27
Mini hop 3	77.27	0.25	0.96	8.52	76.29
Mini hop 4	76.29	0.25	0.95	7.57	75.32
Inbound hop	75.32	15	7.23	0.34	67.95
Totals	N/A	31	19.66	0.34	67.56

Refueling Stations

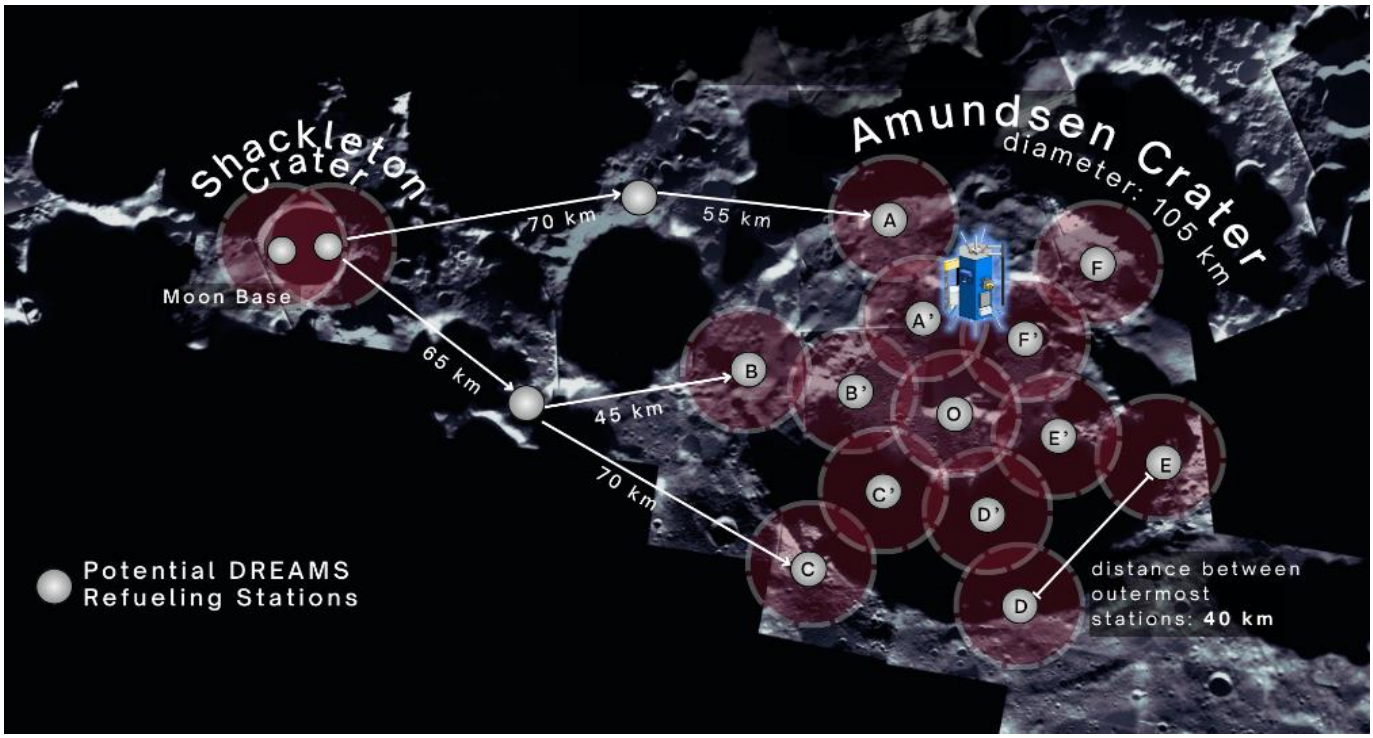


Figure 14. Graphical depiction of potential DREAMS refueling stations

Due to the range of DREAMS as described previously, the following refueling station setup is proposed. In this depiction, Amundsen crater is used demonstratively as the chosen excavation site; however, a similar but slightly modified setup could be used for any other chosen excavation site.

At Shackleton crater, two refueling stations will be placed inside the crater at two parallel locations: one at the inner rim closest to the excavation site, and one on the inner rim directly opposite. This ensures that DREAMS will have the adequate range to both make it over the rim of the crater and arrive at the next destination fuel station. Additionally, it enables the exploration and observation of the surrounding terrain outside of the crater, potentially aiding the Moon base initiative outside of Project DREAMS. After departing from the refueling station situated closer to the excavation site, DREAMS's path diverges, with one path meeting a refueling station above Faustini crater, and the other below. These two refueling stations were placed to avoid the crater for maximum fuel efficiency.

The first path follows into the refueling station above Faustini crater, about 70 km away from the initial refueling station After arriving at the midpoint refueling station, DREAMS will arrive at station A. This path is followed when the goal destination is closest to the outermost

refueling stations A or F. The other path leads to a refueling station situated below Faustini crater. From this point, DREAMS can either arrive at the outermost refueling stations B or C.

Upon arrival at an outermost refueling station (A, B, C), DREAMS can safely travel to any other outermost station (D, E, F), due to the 40 km distance between any two consecutive refueling stations. From then on, DREAMS can begin its drilling cycle around any of the refueling stations, with the radii of the distance allowed for a safe drilling cycle to occur marked in red in Figure 14.

Energy Budget

For any space mission, determining the energy and propellant budget is an essential part of the spacecraft's design. For the studied operational concept, the energy and propellant budget was estimated specifically for the DREAMS hopper due to its role of being an innovative system, dedicated to aviation. For a comprehensive assessment, similar analyses should be conducted in the future for the other components of this operational concept.

The DREAMS hopper uses many systems consisting of cameras, spectrometers and a drill to accomplish its goal in this operational concept. However, hardware was not the only aspect considered, as fuel plays a crucial part of our mission. A master energy equation was derived (see equation (3)) to determine the total amount of energy used by each system, while taking into account operational time and conditional procedures. It is important to note that equation (3) only represents the energy used by DREAMS in one "day" of this operational concept, which is the same as one cycle. The energy equation and the following sections will only account for DREAMS's nominal power usage unless explicitly stated otherwise. The energy budget was calculated for each phase of DREAMS's journey, except for Phases 1, 5, 6, and 7, which do not require energy to operate. All units utilize the International System of Units (SI).

$$E_{used} = (N_H + N_M + N_R)P_{O3D\ LiDAR}t_{O3D\ LiDAR} + N_S(P_{LRAD}t_{LRAD} + P_{NSS}t_{NSS}) + \sum_{j=1}^{N_s} \delta_{S,j}\left(\frac{F_{d,j}d_j}{\eta_D} + P_{motor}t_{D,j} + P_{NIRVSS}t_{NIRVSS,j} + P_{MSolo}t_{MSolo,j}\right) \quad (3)$$

Table 4. Variable definitions and values for equation (3)

Variable	Description and Units (SI)	Numerical Value (applicable)
N_H	Number of long hops (non-dimensional)	1
N_M	Number of mini hops (non-dimensional)	4
N_R	Number of return hops (non-dimensional)	1
P_{system}	Power consumed by a system (W)	-
t_{system}	Operational time of a system (s)	-
N_S	Number of sampling sites (non-dimensional)	5
$F_{d,\,j}$	Drilling force (N)	500 [23]
d_j	Drilling depth (m)	0.5
D	Drill efficiency (non-dimensional)	0.30

In the following sections, each part of equation (3) is split by system and phase, and expanded for a full explanation, including the definitions of all variables (see Table 4).

Scientific Exploration Area

The scientific exploration area (or simply area) is defined as the region where sampling occurs. The area (represented by a letter variable with no subscript, e.g. A, B, C) is roughly equal to 1.0 km and should not be confused with the areas in Figure 14. The hopper will always touch down into a subarea, otherwise known as the first sampling location and is represented by a letter variable with subscript 1, e.g. A_1, B_1, C_1. To keep variables consistent and simple, we defined our area as A and the subareas as A_1, A_2, A_3, A_4, and A_5. One should keep in mind that the variable for area and subarea can change, this is only for the purpose of making a nominal power calculation.

Phase 1: Transit to PSR

The DREAMS hopper begins at ABC (still attached to its lander) on the illuminated rim of Shackleton crater. As the hopper turns on, it will set forth the variable $N_H = 1$, where N_H is the number of long, ballistic hops. This phase will only use one component: propellant. As mentioned in Table 3, the DREAMS hopper will use 8.57 L of fuel on its long hop. Throughout its transit, it will continuously charge its battery for its spectrometers, drill, and cameras via the solar panel on its side until full. As it journeys into the PSR, propellant will be used during landing; however, this amount is negligible, therefore, the final amount of propellant used is 8.57 L and of solar energy used is 0 J.

Phase 2: Descent and Landing

This section covers the general use of O3D LiDAR across all of its applications. O3D LiDAR will operate during every long hop, mini hop, and return hop landing. We will be using the O3D LiDAR system [24]. It will activate for a short amount of time once the altitude is between 20-200 meters for imaging and hazard detection. Since a detailed descent trajectory has not yet been developed, it was assumed the O3D LiDAR hazard detection system would operate for approximately 30 seconds (s) during each descent. Since the terrain inside the PSR is poorly illuminated, O3D LiDAR will be activated during descent to determine the safest landing spot possible that minimizes any damage to DREAMS. From equation (3), O3D LiDAR's energy usage is as follows:

$$(N_H + N_M + N_R) P_{O3D\ LiDAR} t_{O3D\ LiDAR} \tag{4}$$

The energy used by O3D LiDAR ($E_{O3D\ LiDAR}$) is equal to the number of long hops (N_H), mini hops (N_M), and return hops (N_R), ($N_H + N_M + N_R$) multiplied by the power consumed ($P_{O3D\ LiDAR}$) and operational time ($t_{O3D\ LiDAR}$) of O3D LiDAR, as shown below.

$$E_{O3D\ LiDAR} = (N_H + N_M + N_R) P_{O3D\ LiDAR} t_{O3D\ LiDAR} \tag{5}$$

The following covers O3D LiDAR's activation while it descends into the subarea A_1 of a bigger crater (A) during a long hop to the PSR.

The energy used by O3D LiDAR during a long hop ($E_{O3D\ LiDAR,\ long\ hop}$) is equal to the number of long hops ($N_H = 1$) multiplied by the power consumed ($P_{O3D\ LiDAR}$) and operational time ($t_{O3D\ LiDAR}$) of O3D LiDAR, as shown:

$$E_{O3D\ LiDAR,\ long\ hop} = (N_H)P_{O3D\ LiDAR}t_{O3D\ LiDAR} \quad (6)$$

To find the energy used by O3D LiDAR as it descends into A_1, we substituted in the following numbers for each variable: $N_H = 1$, $P_{O3D\ LiDAR} = 70\ W$ [24], and $t_{O3D\ LiDAR} = 30\ s$.

$$E_{O3D\ LiDAR,\ long\ hop} = (1) \times 70\ W \times 30\ s \quad (7)$$

Which then results in the energy used by O3D LiDAR during a long hop ($E_{O3D\ LiDAR,\ long\ hop}$) of 2100 J.

Next, we measured the amount of energy used by O3D LiDAR as DREAMS makes its descent into the following subareas: A_2, A_3, A_4, and A_5. Thus, the following section will cover O3D LiDAR's activation during its descent during each mini hop.

The energy used by O3D LiDAR during a mini hop descent ($E_{O3D\ LiDAR,\ mini\ hop}$) is equal to the number of mini hops ($N_M = 4$) multiplied by the power consumed ($P_{O3D\ LiDAR}$) and operational time ($t_{O3D\ LiDAR}$) of O3D LiDAR, as shown:

$$E_{O3D\ LiDAR,\ mini\ hop} = (N_M)P_{O3D\ LiDAR}t_{O3D\ LiDAR} \quad (8)$$

The amount of energy used by O3D LiDAR during its descents into the subareas after A_1, we substituted in the following numbers for the variables: $N_M = 4$, $P_{O3D\ LiDAR} = 70\ W$ [24], and $t_{O3D\ LiDAR} = 30\ s$.

$$E_{O3D\ LiDAR,\ mini\ hop} = (4) \times 70\ W \times 30\ s \quad (9)$$

Which then results in the total amount of energy used by O3D LiDAR during all of its mini hop descents ($E_{O3D\ LiDAR,\ mini\ hop}$) of 8400 J. We then measured the amount of energy used by O3D LiDAR as DREAMS makes its descent back into ABC.

The energy used by O3D LiDAR during a return hop descent ($E_{O3D\ LiDAR,\ return\ hop}$) is equal to the energy used by O3D LiDAR during its long hop ($E_{O3D\ LiDAR,\ long\ hop}$). The total amount of energy by O3D LiDAR during its return hop descent is 2100 J.

Finally, to determine the total amount of energy used by O3D LiDAR during all descents ($E_{O3D\ LiDAR}$), we took the aforementioned numbers and substituted in [24]:

$$E_{O3D\ LiDAR} = (1 + 4 + 1) \times 70\ W \times 30\ s \tag{10}$$

This returns the total amount of energy used by O3D LiDAR at 12600 J.

Phase 3: Regolith Survey

The regolith survey is the next set of systems that will turn on and operate. However, the fact that it will start at subarea A_1 does not mean the spectrometer and radiometer systems are limited to that subarea. The survey will apply to all of the subareas (A_1, A_2, A_3, A_4, A_5) within a specific area (A). From equation (3), the energy used by the regolith survey is represented by:

$$N_S(P_{LRAD}t_{LRAD}+P_{NSS}t_{NSS}) \tag{11}$$

After completing its transit and safely landing within a PSR, DREAMS will start at subarea (A_1) and begin its initial investigation by using the following systems: LRAD and NSS. The total energy spent on our regolith survey was calculated with the following equation: (E_{survey}) is equal to the number of sampling sites ($N_S = 5$) multiplied by the power used by LRAD (P_{LRAD}) and operation time of LRAD (t_{LRAD}) added to the power used by the NSS (P_{NSS}) and the operation time of the NSS (t_{NSS}), giving us the following addition of $P_{LRAD}t_{LRAD}+P_{NSS}t_{NSS}$, as shown below:

$$E_{survey} = N_S(P_{LRAD}t_{LRAD}+P_{NSS}t_{NSS}) \tag{12}$$

Substituting in the following nominal numbers: $N_S = 5$, $P_{LRAD} = 1.5$ [18], $t_{LRAD} = 3600\ s$, $P_{NSS} = 1.5\ W$ [2], $t_{NSS} = 3600\ s$, into the equation above:

$$E_{survey} = 5(1.5\ W \times 3600\ s + 1.5\ W \times 3600\ s) \tag{13}$$

results in the total amount of energy used by our survey (E_{survey}) of 54000 J.

Phase 4: Conditional Drilling and Analysis

When performing the survey in each sampling location, there is a possibility that DREAMS might not drill and take a sample at that specific location. It depends upon the systems of Phase 3, if they report that the subarea is suitable for drilling. If it finds the presence of hydrogen, its state, and the composition is viable, then the process continues with Phase 4, where a conditional is set up. The conditional will rely on a binary state, where a value of 1 indicates to proceed with operation and a value of 0 indicates to cease the current system operation and move on (this is discussed later). The conditional is set up by the following:

$$\delta = \begin{cases} 1, & \text{target consisting of hydrogen, volatile, and correct composition found} \\ 0, & \text{no suitable target found, cease current operation, proceed to next phase} \end{cases} \tag{14}$$

For consistency, we assumed that the survey was successful and DREAMS would proceed to Phase 5 after Phase 4. Assuming that the survey outputs the binary state of $\delta = 1$, DREAMS will proceed with the drilling and analysis process by using the systems of TRIDENT and MSolo, respectively.

The energy used for drilling and analysis ($E_{drilling\ and\ analysis}$) can be found using the following equation: the energy used by drilling and analysis $E_{drilling\ and\ analysis,\ total}$) is equal to the sum ($\sum$) of all sampling sites ($N_s = 5$) where drilling occurs, represented by the binary conditional $\delta_{S,j}$. For each site, (j), the total energy includes the mechanical drilling energy calculated as the drilling force ($F_{d,j}$multiplied by the drilling depth (d_j) and then divided by the drill efficiency (η_D); the motor power (P_{motor}) is multiplied by the drilling time ($t_{D,j}$); the NIRVSS instrument power (P_{NIRVSS}) multiplied by its operation time ($t_{NIRVSS,j}$); and the MSolo instrument power (P_{MSolo}) multiplied by its operation time ($t_{MSolo,j}$).

$$E_{drilling\ and\ analysis} = \sum_{j=1}^{N_S} \delta_{S,j} \left(\frac{F_{d,j} d_j}{\eta_D} + P_{motor} t_{D,j} + P_{NIRVSS} t_{NIRVSS,j} + P_{MSolo} t_{MSolo,j} \right) \quad (15)$$

Substituting in the following nominal numbers $\delta_{S,j} = 1$, $N_s = 5$, $F_{d,j} = 500\ N$ [23], $d_j = 0.5\ m$, $\eta_D = 0.30$, $P_{motor} = 325\ W$ [2], $t_{D,j} = 1800\ s$, $P_{NIRVSS} = 29.6\ W$ [2], $t_{NIRVSS,j} = 3600\ s$, $P_{MSolo} = 34\ W$ [26], $t_{MSolo,j} = 3600\ s$:

$$E_{drilling\ and\ analysis} = \sum_{j=1}^{5} 1 \left(\frac{500\ N \times 0.5\ m}{0.30} + 325\ W \times 1800\ s + 29.6\ W \times 3600\ s + 34\ W \times 3600\ s \right) \quad (16)$$

This results in the total amount of energy used by drilling analysis ($E_{drilling\ and\ analysis,\ total}$) of 4,073,966.67 or 4.07×10^6 J.

Phase 5: Mini Hops

After the survey, drilling, and analysis processes have finished at a certain subarea from A_1 to A_4, DREAMS will turn off all systems as it prepares to move toward making a mini hop to the next subarea. Subarea A_5 is going to be excluded from making any mini hops because it is considered to be the end of the sampling process; this will be covered in Phase 6. For all four mini hops ($N_M = 4$), the only system used will be propulsion. As previously mentioned in Table 3, the amount of propellant used during each mini hop is approximately 1 L. The total amount of propellant used by all 4 mini hops is 3.86 L. After each mini hop, we redirect back to Phase 2 of descending.

Phase 6: Return

After all 4 mini hops ($N_M = 4$) and 5 sampling sites ($N_S = 5$), the DREAMS hopper will shut down every system as it transitions towards Phase 6, returning to ABC. According to Table 3, the amount of fuel used by the DREAMS hopper is 7.23 L. Our return hop will follow the same procedures as both the long and mini hops did by turning all systems off and focusing its attention on propulsion only. Since it has a solar panel, it will also charge its electrical systems (like NSS, NIRVSS, and TRIDENT) until it reaches its distance of 200 m from ABC where it will then transition back to Phase 2.

Phase 7: Refuel, Recharge and Communication

Once the return to ABC has been completed, DREAMS will refuel its monopropellant hydrazine thrusters while simultaneously recharging its electrical systems via the solar panel on its side. During this stage, DREAMS will have every system turned off and begin its communication phase. The communication phase will consist of having DREAMS relaying information about which sampling site was the most optimized for additive manufacturing to T-REx. Once T-REx receives this information, it will then excavate the regolith out of that area to be used for our 3D printing. After the communication phase, DREAMS will finally go dormant until the next cycle of operation.

Total Energy Used

After calculating the energy used by each system, we put together the final equation for the total energy used by DREAMS per one operational cycle, simplified from equation (3).

$$E_{used} = E_{O3D\ LiDAR} + E_{survey} + E_{drilling\ and\ analysis} \tag{17}$$

Substituting in the nominal numbers from each set of systems:

$$E_{used} = 12{,}600\ J + 54{,}000\ J + 4{,}073{,}966.67\ J = 4{,}140{,}566.67\ J \tag{18}$$

We return the total amount of energy used by the DREAMS hopper of 4,140,566.67 or 4.14×10^6 J.

<u>End of DREAMS Cycle</u>

This concludes stage one of Project DREAMS and marks the transition from the DREAMS to the T-REx cycle.

<u>Comparison of DREAMS to Pre-existing Systems</u>

The biggest influence on the DREAMS hopper is undoubtedly the Micro-Nova hopper. Table 5 shows a comparison between the two hoppers.

Table 5. Comparison between DREAMS and the Micro-Nova hopper. *estimation **[27]

	μ-Nova	DREAMS
Mass	45 kgs*	88 kgs
Height	1.0 m**	1.2 m
Fuel Capacity	6 liters*	20 liters (additional 3 liters for reserve/ attitude control)
Estimated Range	25 km**	75 km one-way, 15 km round trips (accounting for mini hops)
Basic Capabilities	Hopping, Surface Analysis	Hopping, Drilling, Surface & Excavated Soil Analysis

There are some notable differences between the two hoppers, the largest one being the difference in mass. DREAMS is nearly two times as heavy as Micro-Nova and 20% taller. To compensate for this, DREAMS has almost four times as much fuel onboard. This increase in fuel is the main factor for DREAMS' range being larger than Micro Nova's. Additionally, DREAMS and Micro-Nova serve different purposes; Micro-Nova was supposed to be used as a testing device and proof of concept on the moon as well as making short hops into PSRs, while DREAMS is a long-range and drilling hopper [28].

II. T-REx

The Terrain-adaptive Regolith Extractor (T-REx) rover will be used primarily to collect and transport regolith from a chosen excavation site back to ABC, where regolith-based 3D printing will then occur after going through a process of refinement and separation.

Introduction

The T-REx rover takes inspiration from the Infrastructure Pilot Excavator (IPEx Rover), which is being developed by the Kennedy Space Center. The IPEx is equipped with four main

subsystems which aid with autonomous driving, navigation, and excavation: The Camera and Dust Mitigation System, the Mobility System, the Regolith Delivery System, and the Thermal Control System.

The IPEx rover's Mobility System, consisting mainly of large wheels and wheel actuators, enables traversal at a nominal driving speed of 30 cm/s. Additionally, the IPEx Rover can only traverse rocks and other obstacles of up to 7.5 cm in height and is limited to inclinations of up to 15°, due to the absence of a suspension system. The Regolith Delivery System, which collects regolith from the lunar surface using counter-rotating bucket drums, can collect, carry, and deposit loads of up to 30 kg of regolith per excavation cycle [3].

While Project DREAMS's goal for the purpose of the rover remains the same, its usage differs. While the IPEx rover was designed with extremely short-distance travel in mind (70 km total traversal over an 11-day period, with excavation sites and unloading sites being around 100 m apart from each other), our rover requires stability over long-distances to enable safe traversal between two craters, potentially 100 km or more away [29]. In order to match the needs of our project, we will utilize IPEx's Regolith Delivery System in our proposed rover, the T-REx rover, while changing the existing Mobility System to have more stability in obstacle and long-distance traversal.

Design Overview

Active Gimbal Suspension

Excavating regolith to extract water and other concentrated minerals requires rovers to dig up and carry heavy payloads to be transported to the site of separation or build. However, the current payload transport system IPEX uses a simple rigged suspension system utilizing skid steering, often limiting the terrain toleration to gradual inclines and smooth land. The current design poses as strongly unrealistic for the operations planned. Conversely, rovers equipped with active suspension systems excel at unplanned obstacle navigation through advanced locomotion. With such benefits comes the high risk of sensitivity to offset load distributions and unintentional dust collection (Figure 15*)*.

Inspired by ERNEST's Active Gimbal Suspension (AGS), our modification consists of two independent motion mechanisms designed to maximize the rover's mobility. Equipped with a clutch mechanism, the rover allows the bogie to switch between actuated and free-motion

modes to advance the machine over challenging uneven terrains. Additionally, the Active Gimbal Suspension (AGS) enables articulation about both the yaw and roll axes. This suspension system allows the rover to perform side-to-side (yaw) and longitudinal (roll) maneuvers. The wheels are designed to carry and shift the weight allowing T-REx to have wheel-walking abilities [4].



Performance Metric	IPEx (Fixed wheels)	T-REx (Active Gimbal Suspension)
Maximum Speed (Flat Terrain)	**0.30 m/s**	**0.30 m/s**
Average Speed (Rocky Terrain)	**0.18 m/s**	**0.26 m/s**
Obstacle Traversal Speed	Low	High
High-Centering Risk	High	Low
Wheel Ground Contact	Moderate	Excellent
Traversability	Good	Excellent

Figure 15. The table compares the IPEx and T-REx's performance metrics of suspension systems

Computer System Adaptabilities

Using NASA's most recent rover, in development since 2022 and with major first field testing done in March 2026, the Exploration Rover for Navigating Extreme Sloped Terrain (ERNEST) provides newer and more efficient mobility in challenging terrain. ERNEST's speeds have proven to be 10 times faster than NASA's Perseverance Rover with its flexible suspension. The system utilizes RL-based locomotion using Reinforcement Learning algorithms to traverse complex terrain. This behavior allows robots to determine when to speed up through obstacles using motor skills and precisely timed and coordinated sequences [4].

Through its specialized RL training and policy consolidation, ERNEST's Active Gimbal Bogie serves as the perfect candidate as it is designed to adapt and memorize the different types of terrains it may encounter on its journey. Even as the paths may change due to weathering and electrostatic sandstorms, the RL system will continue to learn how to adapt to the new challenges

set on the road ahead. The rover can relay this information to future vehicles that may travel similar paths in the given areas [30].

Camera System

Due to the new suspension system, the camera system on the current IPEx model will become extremely unstable and inaccurately track the terrain into a 3D modeled design. The original design consists of 4 mono cameras and 2 stereo camera pairs used for situational awareness and localization (Figure 16). The stereo cameras are specified for visual odometry and hazard detections, while the mono cameras will track the location of the rover [3, 4]. Since the camera system is attached directly to the body, they will experience all of the movements and shaking due to the movements required for T-REx to accurately drive over certain terrain [3].

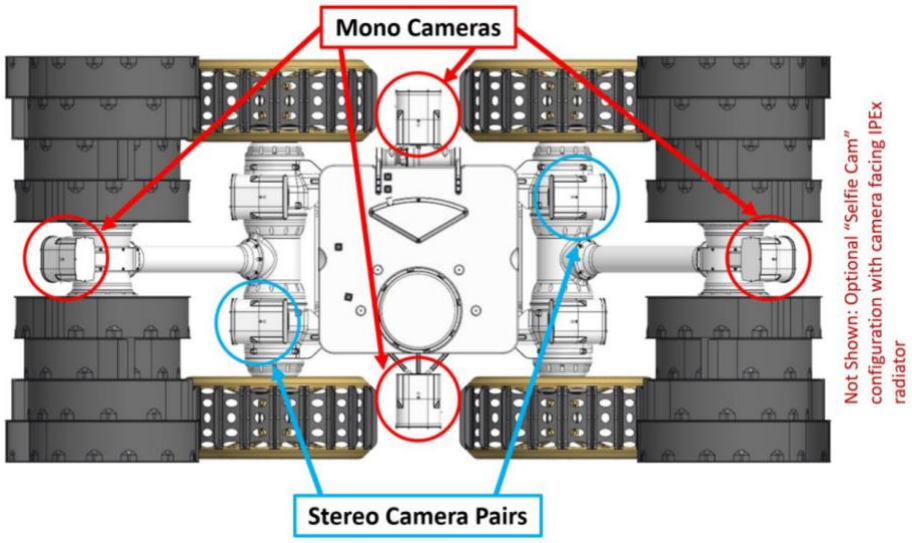


Figure 16. Camera anatomy of IPEx Rover (inspiration)

In order to combat this, the redesign follows ERNEST's current model as well as other Mars rovers. The new camera system only consists of side perception cameras, stereo navigational cameras and LiDAR (not to be confused with the O3D LiDAR), all on a rotational rig attached to a 4-foot pole (Figure 17). The camera system is primarily used to take videos, aid in localization and 3d tracking for the rover to analyze and decide on how to go about the obstacles ahead [4].

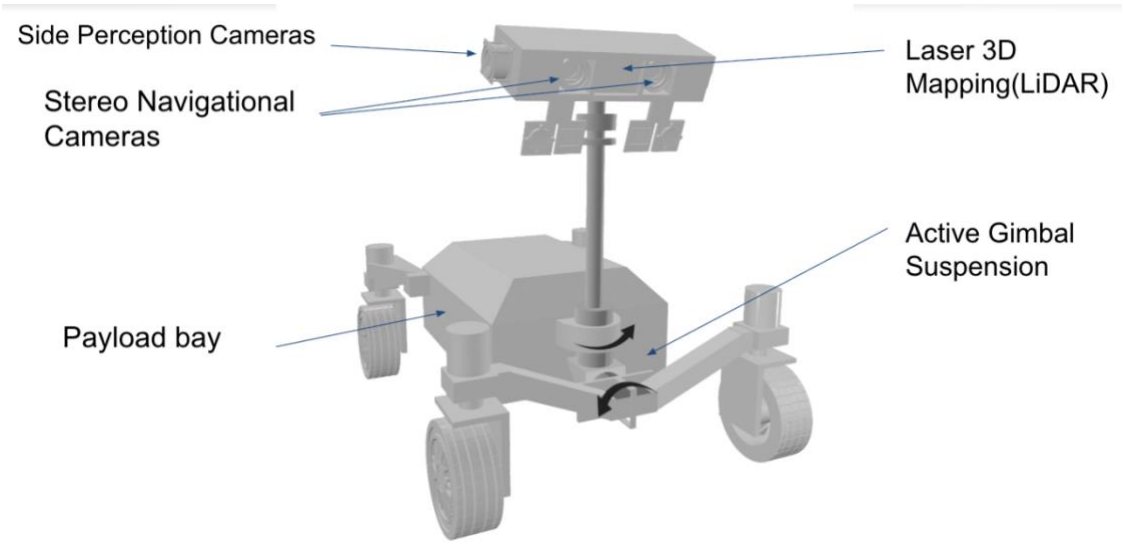


Figure 17. CAD model of T-REx external structure

Payload Bay

Looking to combine the Active Gimbal Suspension with IPEx's bucket drums, the rover comes with complications on the aspect of spacing and placements of each tool. This introduces the concept of the payload bay. The main body of the rover will function as a storage unit for the 4 large bucket drums during travel, while the placement of the wheels will remain the same as the current ERNEST model (Figure 17).

Within the payload bay (see Figure 18) the bucket drums will be held in place by extendable arms on both sides. During excavation, two mechanical sliding doors will open after the wheels lock in place allowing the bucket drums to be lowered onto the ground while spinning in counter rotational directions to prevent moving the rover from the specific excavation spot.

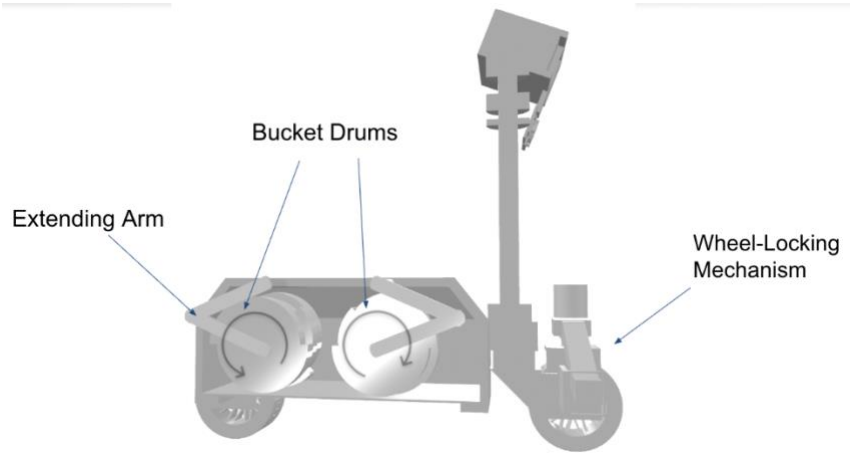


Figure 18. CAD model of T-REx Internal Structure

Navigation

Scenario of use for T-REx Rover

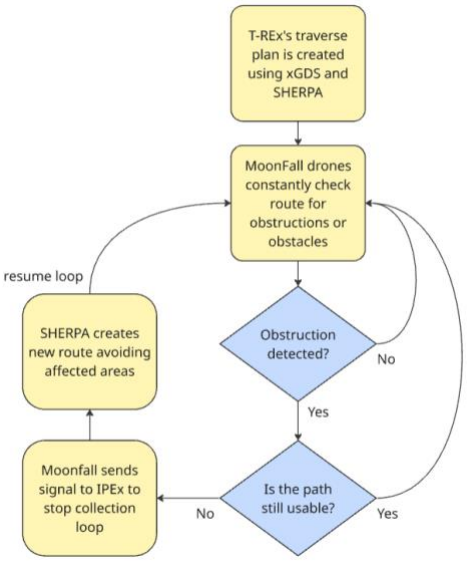


Figure 19. Flowchart representation of T-REx's path planning process

As shown in Figure 19, after DREAMS chooses an optimal excavation site through extensive drilling and testing, T-REx's traverse path from the area near the illuminated rim of Shackleton crater (where the ABC will be located) to the chosen excavation site within the PSRs of Aitken, Amundsen, or Shackleton crater is created using SHERPA, with xGDS being used

only if deemed necessary. SHERPA takes the various conditions of the lunar surface and T-REx's mechanical constraints into account while creating this path. After a traverse plan is created, simulated, and approved by SHERPA, T-REx is sent on the path to begin the process of regolith collection.

Natural occurrences on the moon, such as electrostatic dust storms and lunar avalanches, can create obstructions in the traverse path that could potentially damage T-REx's machinery or prevent the collection loop from continuing. To prevent this, while T-REx continues the loop of collecting regolith from the excavation site and depositing the regolith back to the ABC, MoonFall drones will be deployed periodically to observe the traverse plan that is currently being used. Using its optical cameras, MoonFall detects obstacles in the path, and determines whether these obstacles prevent T-REx from safely traversing the path. If the path is considered usable, MoonFall returns to ABC to rest until the next check is due.

If the obstacles discovered deem the path unfit for T-REx to traverse safely, MoonFall immediately communicates with T-REx to stop the collection loop and return to ABC. While the collection loop is paused, SHERPA considers the new conditions of the surface to create a new route avoiding the areas affected by obstructions. After SHERPA creates a new viable path, T-REx is alerted to continue regolith collection, now using the new traverse plan. This new traverse plan will continue to be followed until MoonFall detects an obstruction, leading to the repetition of this cycle.

MoonFall Drones

The MoonFall drones will be used to monitor the safety and usability of chosen traverse plans to ensure the longevity and sustainability of the T-REx rovers and the system as a whole.

MoonFall is being developed by NASA's Jet Propulsion Laboratory as a part of the Moon Base Initiative.

The drones are equipped with up to 10 high-definition optical cameras, which take high-resolution images of the moon's terrain to be used in MoonFall's Lunar Dashcam imaging system. The Lunar Dashcam imaging system is able to produce high-resolution digital terrain maps. A laser retroflector array allows for precise location of the drones, allowing for accurate communication between the drones, T-REx, and humans at ABC [3].

MoonFall's other systems include a neutron spectrometer for subsurface water detection and a separate spectrometer for radiation detection. For the purpose of path planning and

obstacle detection for T-REx, these systems will remain dormant unless specific conditions cause them to become necessary.

Path Planning Software

SHERPA

The Systems Health Enabled Real-time Planning Advisor (SHERPA) was developed as an Artificial Intelligence system to be used for NASA's Volatile Investigating Polar Exploration Rover (VIPER) mission. In this system, it will be adapted for usage with the T-REx Rover.

SHERPA processes a variety of factors including but not limited to the Moon's surface terrain and the limits of the rover, such as range, refueling, and traverse angle limitation [4]. To synthesize a traverse plan prior to mission launch, SHERPA considers the above factors to develop several options of traverse plans. It then runs thousands of mission simulations and assesses risks primarily using Markov decision processes (MDPs) and partially observable Markov decision processes (POMDPs) [30]. Based on these simulations, a traverse plan can be finalized. After launch, SHERPA uses problem solving skills to adjust traverse plans in real-time based on new information.

xGDS

The Exploration Ground Data Systems (xGDS) is a suite of web tools that synchronizes collected information (e.g. photos, samples, and observation notes) with time and location to support decision making, including traverse planning. xGDS's Plan Editor allows for the creation of traverse plans on a map, with distance and duration updates based on user input. Other features include plots based on discrete instrument data and continuously streamed data, ability to annotate still images from camera or video capture, and ability to organize collected samples by metadata using QR-coded labels [31].

While SHERPA will act as the primary software used for path planning, xGDS will be used in cases where human intervention is required or SHERPA results are considered unusable due to special circumstances.

Conclusion

T-REx proves to have the optimal functionality for the collection and transportation of regolith required for the further building and construction plans of the Moon Base Initiative.

IPEx was built with short distance traverse in mind, while Project DREAMS's Concept of Operations demands for longer distance traverse, potentially transporting regolith across the diameters of craters or even between separate craters; these requirements led to the creation of the T-REx rover. The T-REx rover's movement systems allow for the transport rover to last the trip with lower chances of the rover breaking or getting tipped over. T-REx uses the latest model of a suspension system, to have the highest efficiency moving to each digging site. Combined with the security of traverse ensured by MoonFall drones, T-REx is able to traverse any terrain and distance on the lunar surface with ease.

As T-REx is designed for longer distances than IPEx, its energy requirements would be considerably larger than those of IPEx. Due to time constraints of the program, energy requirements associated with the increased range of T-REx were not evaluated; however, an energy assessment similar to that of DREAMS would be necessary along with further refinement and implementation of the design.

III. Lunar Auger Dryer ISRU (LADI)

Created by NASA's Johnson Space Center, the Lunar Auger Dryer ISRU, or LADI, is used in our workflow to process regolith in between the stages of excavation and LPBF printing. After the DREAMS hopper locates a suitable dig site and the IPEx rover transports regolith, the LADI extracts water and volatiles from the material that can be used in other systems. This allows the regolith to be useful for the overall sustainability of the project. Afterwards, the regolith will be powdered and sent for LPBF printing.

The LADI (see Figure 20*)* is a stationary processing machine designed to utilize regolith from the permanently shadowed regions of the lunar poles that are rich in ice content [17]. Regolith is put into the system's inlet machine hopper, sorted to remove large chunks and particles, and then fed into the auger dryer. The regolith that passes through the auger casing is heated in order to release water vapor, which is then stored in a cold trap where it can be collected as ice and electrolyzed for volatile extraction in a different system [17]. The remaining dried regolith can be utilized for LPBF printing.

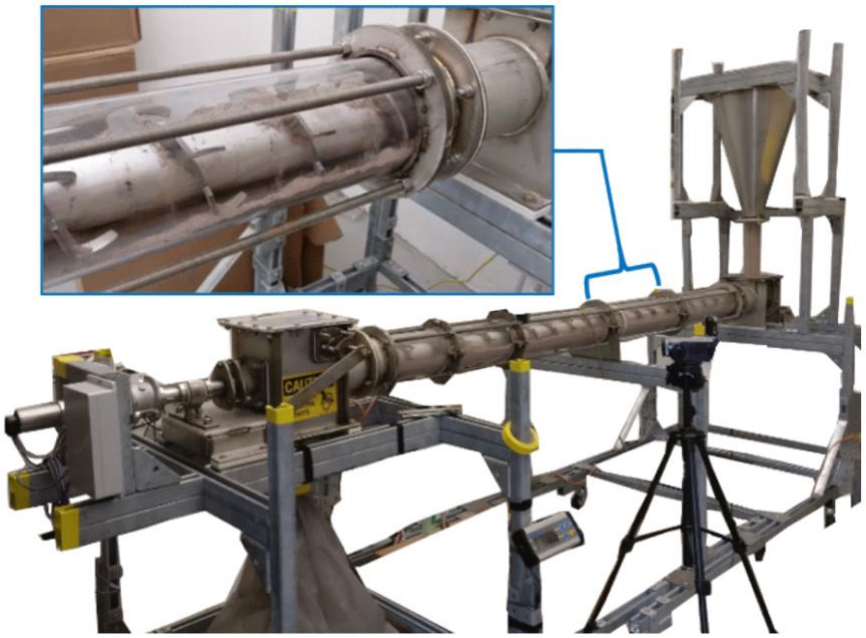


Figure 20. LADI auger dryer test system used for icy regolith processing [17]

Specifications

The system requires the regolith to be delivered in a controlled manner before it reaches the auger dryer. The inlet hopper contains a size sorting stage that removes oversized rocks which could jam in between the auger conveyor and the casing. This is vital as the auger dryer relies on a maximum particle size of 2 mm to reliably extract water content from the regolith without harming the system [17].

The LADI was created with several design assumptions in mind to estimate the system's regolith processing requirements. The dry regolith bulk density is assumed to be 1300 kg/m^3 in testing [17]. The auger dryer is assumed to be able to process a maximum particle size of 2 mm [17]. Furthermore, regolith is assumed to have an average water concentration of 5% wt, meaning that water weight makes up 5% of the regolith's mass [17]. LADI's estimated water extraction efficiency of 75% illustrates that most of this water content will be collected and recycled for other use cases around ABC [32, 33]. Due to the varying conditions of regolith, these numbers serve as assumptions and are expected to show differences when compared to the regolith properties of authentically lunar soil. The conditions will be verified and confirmed by the DREAMS hopper as it visits potential excavation sites.

LADI is able to trap the water vapor while allowing a continuous stream of regolith to be passed through the auger. This is achieved through tightly packing the regolith at the inlet and outlet of the auger dryer [17]. The packed regolith acts as a soil plug and prevents the water vapor from travelling back up to the hopper or out towards the exit [17]. Using the regolith itself to seal the system allows for decreased energy consumption and less moving parts that can break.

The heating system is designed to prevent the formation of liquid water when processing regolith. Rather than melting the ice into water and then water vapor, the auger dryer heats regolith so that the ice sublimates directly into water vapor [17]. Formation of liquid water could lead to mud forming from the mixture of regolith and water, increasing the possibilities of the auger clogging and lengthening the process overall.

Connection to LPBF printing

In our concept, the LADI serves as a regolith processing system that extracts water content and volatiles, resulting in dried regolith. The water can be utilized for different ISRU needs, whether it be for human consumption or for breaking down into hydrogen and oxygen that can be used for other systems in ABC. The dried regolith must not be assumed to immediately be LPBF printer ready. The material will need to be fragmented and completely powdered in order to ensure the feedstock is printer ready.

IV. Laser Powder Bed Fusion Printing

Laser Powder Bed Fusion (LPBF) is an innovative 3D printing technique that forms structures by fusing powdered material layer by layer. Within this process, a thin layer of powder is set onto a build platform while a laser goes over selective areas and fuses the material together based on a 3D model. Once the layer is completed, another layer of powder is set out onto the build platform and the process is repeated [14]. In this concept, a LPBF 3D printer specialized for regolith is the final stage of the workflow after LADI processing and powder preparation.

Specifications

LPBF can be used to produce protective components that will support the construction of the ABC. Instead of printing the whole living module, the LPBF system will be able to print the surrounding construction materials, such as bricks and shielding tiles that can protect the pressurized living module. These parts provide insulation, protection from radiation, and micrometeorite shielding. In addition, LPBF could be used to create handier items that improve quality of life around ABC [6]. Some examples are sample trays, equipment mounts, tool replacements, part replacements, cable guides, and much more (see Figure 22).



Figure 21. Example of a 3D-printed tool [41]. A regolith-adapted LPBF system could produce similar replacement tools and support parts

LPBF is better suited for an ISRU-style lunar base because it can use powdered regolith to produce components without needing a binder or filament sourced from Earth. Standard 3D printing often takes filament or a binder-infused material as a feedstock, which would increase the number of materials necessary for the mission and not be sustainable. LPBF, however, can fuse regolith powder sourced from the moon to construct parts. This helps to decrease dependency on Earth, which is in line with our ISRU goals. Since the feedstock is based on lunar regolith, LPBF provides more self-sufficiency to the overall system. Damages and repairs to regolith 3D printed construction could be easily replaced and improved upon. However, LPBF requires careful powder preparation and precise settings based on the regolith composition. The powder feedstock must show consistency in particle size, and printer settings require careful management of laser power, layer thickness, hatch spacing, and scan speed in order to produce high-quality results [34]. Settings have been perfected on Lunar Mare Simulant-1 (LMS-1); however, they may not yield the same results when performed on authentic lunar regolith feedstock. LMS-1 lunar mare regolith is modeled after optimal regolith conditions that are rich in

basalt content [34]. The regolith found on the moon should not be expected to perfectly mimic these conditions. Tailored settings will have to be adapted based on the analysis of on-site regolith done by DREAMS and lab testing.

Impact

LPBF gives ABC a way to sustain itself by using materials that are made available from the moon's environment. Instead of relying on Earth for broken parts or replacements, ABC could manufacture components on demand as needs arise. Having this system in place would support future long-term operations on the moon. Any parts that are damaged or unusable could be crushed and powdered again to be put back into the LPBF printer for lower-importance parts, adding a layer of reusability to our operation.

Impact and Conclusion

Impact

As a whole, Project DREAMS creates a long-lasting system enabling sustainable life on the moon by significantly reducing the costs and energy required to maintain sustained human presence on the moon, while furthering the ongoing exploration of the moon. Project DREAMS's systems can be used to create objects tailored individually to serve a variety of purposes, including replacement parts for machinery and structures for human habitats, as seen in Figure 22. With the implementation of Project DREAMS, human habitation of the moon becomes a reality, affecting the entire next generation of mankind.

With the DREAMS hopper, humans can gain extensive knowledge of previously uncharted and unobserved parts of the moon (especially PSRs), with spectrometers surveying information such as surface temperature and radiation. Most importantly, DREAMS creates opportunities for the discovery of volatiles in the regolith, including hydrogen and water, potentially completely altering the trajectory of mankind's presence on the moon. Our extensive research into the optimization of DREAMS' range and fuel capacity ensures that research operations remain as efficient as possible, while providing the basis for the further development of moon hoppers in the future. T-REx rover's advanced regolith collection and mobility systems provide the foundation for in-situ resource utilization on the moon, made possible through LPBF printing. Combined, these systems make sustainable living on the moon possible; the need for

the shipment of Earth-bound materials and resources decreases drastically, reducing the carbon footprint of the Moon Base initiative (see Figure 23) and expediting the realization of its goals.

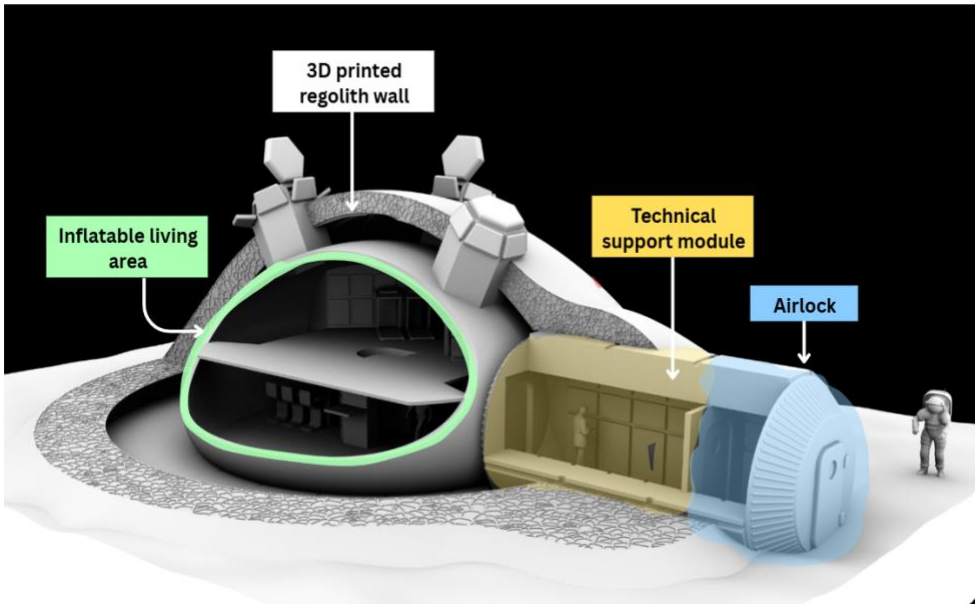


Figure 22. European Space Agency's vision for a Moon base. Photo: ©ESA [40]

Conclusion

Our vision and goal of Project DREAMS is to provide an aviation-based technological solution for building self-sustaining habitats to support long term human presence on the moon. Regolith is an excellent barrier since it absorbs radiation, so it can provide thermal and radiation protection for humans and equipment in space. Although we encountered a lot of challenges while designing the DREAMS hopper and T-REx rover, we were able to find innovative solutions in the limited time and scope of this project. There is still room for improvements to the design of the hopper and the rover, and the ever so important question of choosing the optimal crater based on distance and regolith composition still remains open to interpretation. Despite the limitations and time constraints, we were able to propose a viable solution of 3D printing bricks, slabs, replacement parts, and on demand tools for future missions. Our proposed operational concept can also be expanded to develop a fleet of DREAMS hoppers and T-REx rovers to meet the needs of the future. Overall, we hope to inspire the next generation of innovators and would love to see our dreams take a flight.

Future Work

Making DREAMS Come True

The DREAMS hopper is a system consisting of spectrometers, cameras, and a drill. Multiple measures were considered and altered to make our hopper come true. One such example is the downsizing of the TRIDENT drill from its original height of 1.0 m down to 0.5 m. Although shrinking the drill size might be easy, the challenge lies within attaching the drill and developing the new design. A conservative route must be followed in compliance with real-world situations including but not limited to preliminary design, propulsion integration, software matching, environmental qualification, and final preparations. Weighing in these factors, we predict a developmental time of approximately seven years for the DREAMS hopper. This represents the amount of time for DREAMS to be sent to the Moon if development began in 2026, aiming for a likely 2033 launch date. Since this is a concept, aerodynamics and engineering were not considered during the creation of the DREAMS hopper. Therefore, the design, along with the goal of Project DREAMS, is subject to change.

The Future of DREAMS

The range of DREAMS is one of the most important factors of the system, as a longer range can cut down on necessary refueling stations and reduce cost and energy overall. The two easiest ways to increase range are undoubtedly increasing fuel and decreasing weight. However, increasing fuel costs space and energy, and it also has diminishing returns as increasing fuel increases weight as well. Additionally, decreasing weight is not possible on DREAMS, as every system on DREAMS is essential to its functionality and role in the mission. However, there is still a lot of potential for improvement. One way to do so would be technological innovations to DREAMS systems. As seen earlier in the paper, range increases quadratically with specific impulse. The range and drilling estimations for DREAMS were made using the latest technology. The monopropellant hydrazine engines we studied had a specific impulse of about 220 isp [25]. Specific impulse is a performance measure of hydrazine engines, and if this could be improved from 220 to 230 isp, the range would increase by 9.3%. There are other ways to increase the range of DREAMS without new technology as well; for example, optimized flight paths may increase the hopper's range. But perhaps the best innovation-driven pathway to increase hopper range is through decreasing takeoff time. Takeoff is the most fuel-inefficient part

of any vertical flight; the craft is at its heaviest, takeoff is directly opposing gravity, and simple kinematics shows that acceleration from stop is the least efficient per unit of distance. As an example, during the Apollo missions, Saturn V used a whopping 43% of its fuel in the first 67 km of launch [32], burning 40 tons of fuel per second instantaneously after launch [33]. Therefore, we present two possible future innovations to reduce fuel usage in takeoff while still accelerating to the same speed.

SpLASH

One of the innovations we propose is SpLASH, or Spring-Loaded Assistive Suspension for Hopper. Currently, moon hoppers like μ-Nova and MoonFall have straightforward landing legs; however, the IM-2 lander Athena does have geometric support to assist on landings [5, 27]. However, even the IM-2 geometric landing leg design does not include assistance for takeoff. SpLASH would store solar energy and transfer it to load springs in the landing legs; these springs would then release on takeoff, providing additional thrust to DREAMS. However, this would likely add weight to the hopper, which may offset the added range given by SpLASH. Further research needs to be completed to fully develop SpLASH and make it beneficial for the hopper.

Refueling Station Launcher

One way to eliminate the extra weight a suspension system would provide is to put the external acceleration system on the refueling station rather than DREAMS. The concept would be similar to the catapult system on an aircraft carrier used to help fighter planes take off, but vertically rather than horizontally. Many of these catapults use either steam-powered or electromagnetic propulsion to launch the aircraft [35], and we would be forced to use the latter as the moon has no atmosphere. This extra acceleration will save fuel and increase range. However, this would be a more complex design, and the landings would have to be very accurate.

Table 6 shows the benefits and drawbacks of the two assistive launching systems compared to the current system.

Table 6. Pros and cons of SpLASH and Refueling Station Launcher

Landing System	Pros	Cons
SpLASH	- Predictable force on takeoff - Absorbs impact on landing	- Heavy - Requires solar power/ other powering mechanism - Complex design
Refueling Station Launcher	- No added weight to DREAMS - Simple power/energy transfer - Most thrust	- Requires accurate landing - Higher-cost, complex design/implementation - Only available from refueling station

The Hydrazine Challenge

When it comes to monopropellant fuel, hydrazine is the most common. It chemically decomposes when flowing through a catalyst bed, producing thrust [25]. Its advantage lies in the fact that it does not need an oxidizer. However, there are a couple of issues with using hydrazine as fuel. The biggest one is that it is not easy to self-sustain. Hydrazine has the chemical composition N_2H_4, and its two elemental components, nitrogen and hydrogen exist in very small amounts in lunar regolith. While hydrogen does exist in water and can be identified by NSS, nitrogen exists in such trace amounts that it is currently not possible to produce hydrazine on the moon using only in-situ resources. Even if it is possible to obtain the necessary nitrogen and hydrogen, creating hydrazine is another matter. There are three main methods to make hydrazine: the Raschig process, the ketazine process, and the peroxide process. The details of these processes are beyond the scope of this project, but the important unifying factor is that all three of these processes begin with ammonia, which has chemical formula NH_3, as the main reactant [36]. In theory, however, we could make hydrazine on the moon given the necessary components, and ammonia is more stable and easier to transport than hydrazine. Even if the hydrazine is synthesized on the moon, we would still need a way to transport it to all the refueling stations. Besides, we would need a significant amount of hydrazine in the first place. 20 liters is equivalent to about 5.3 gallons, and that is used on every drilling cycle or one-way hop.

While this is out of scope for our paper, our current solution to this would be to transport ammonia and the necessary catalysts to the moon from Earth using a transport spacecraft or on board other lunar voyages. While this does not make for a fully self-sustaining system, ammonia will be easier to transport than building components or replacement parts. Further research and development would need to be done to address this hydrazine challenge, to either figure out a way to transport ammonia or hydrazine conveniently or synthesize it using in-situ resources. From a systems perspective, we would need to figure out how to get this fuel to the refueling station, whether that involves a large network of pipes, separate delivery system, or another innovative technology. Overall, for a roadmap for Project DREAMS to be implemented, this challenge would serve as a possible next step.

T-REx

The Terrain-adaptive Regolith Extractor (T-REx), a cross-hybrid between ERNEST and IPEx rover, was created for efficient travel of the lunar surface and excavation of regolith material. While the paper presents the overall concept covering the general operational design, for future works and developments, several factors will have to be considered. We generally looked at solar energy powering computer systems, the design of mesh metallic wheels, and determining how stable the rover will be to carry the weight and traverse successfully. Several design parameters are undetermined as ERNEST went through its first major testing in the Colorado Desert in March 2026, therefore majority of the information is not publicly released to reference. As a result, engineering assumptions are made to bridge the gaps between the available data.

In the case of the actual implementation of our operational concept, it is suggested to use multiple T-REx rovers to ensure that an adequate amount of regolith is being supplied to the 3D printing station to meet its demands based on the part currently being manufactured. This paper does not propose an exact number of T-REx rovers. In this scenario, the path planning process could be modified to create traverse plans for multiple groups of T-REx rovers, preventing cross-group intersection while still maintaining the safety of the traverse plans (avoiding obstacles, obstructions, and steep inclines).

Communications

Project DREAMS planned to model our communications after the IM-2 mission. Partnered with Intuitive Machines, Nokia Bell Labs' Lunar Surface Communications System (LSCS) initiated a 4G/LTE "Network in a box" placed on the lunar lander that would have the ability to communicate to two additional lunar vehicles. Even if the IM-2 mission failed after the Athena Lander tipped over, the mission was deemed successful for 25 minutes before losing power on the moon [37, 38]. This trial run may further help engineers to develop a fully functioning communication system on the moon. For Project DREAMS, the connection would have to work between the lunar lander, the DREAMS hopper, T-REx rover, MoonFall drones, and further 3D printing equipment like LADI and the LPBF printer itself. The communication system would allow for fully autonomous operations by machine.

Appendix

Derivation For Range Equation (see equation (1))

We are solving for r, and r is the total x-distance traveled. We are going to break this x-distance up into two components: the time period when the engines are on and the time period when the engines are off. Let any variable with subscript 1 indicate the time period when the engines are on and any variables with subscript 2 indicate the time period when the engines are off (in other words, projectile motion). Thus, we begin with equation (A1), as seen below:

$$r = x_1 + x_2 \tag{A1}$$

Now we need a couple of other equations. Equation (A2) represents the specific impulse equation, which is a measure of how much fuel the engines use per Newton of thrust. The M variable indicates mass flow in kg/s, and the g_0 variable indicates Earth's gravity, 9.81 m/s^2, as specific impulse is a relative measurement. Equations (A3), (A4), and (A5) are derived from the second kinematics equation. Equations (A6) and (A7) are derived from the first kinematics equation. Equations (A8) and (A9) relate to time period 1 and are derived using a force diagram and Newton's Second Law of motion. Equation (A10) uses equation (A2) to convert the rate of fuel usage to the time it takes to burn through all the takeoff fuel. The coefficient of 1.021 before L converts kilograms of hydrazine to liters, as hydrazine has a density of 1.021 g/cm^3. Equation (A11) is derived using the second kinematics equation and the quadratic formula.

$$I_{sp} = \frac{F}{M \times g_0} \tag{A2}$$

$$y_1 = 0.5 a_y t_1^2 \tag{A3}$$

$$x_1 = 0.5 a_x t_1^2 \tag{A4}$$

$$x_2 = v_x t_2 \tag{A5}$$

$$v_y = \left(a_y t_1\right) \tag{A6}$$

$$v_x = (a_x t_1) \tag{A7}$$

$$a_y = \left(\frac{\frac{F\sqrt{2}}{2} - 1.622m}{m} \right) \tag{A8}$$

$$a_x = \left(\frac{\frac{F\sqrt{2}}{2}}{m} \right) \tag{A9}$$

$$t_1 = \left(\frac{I_{sp} \times 9.81 \times 1.021L}{F} \right) \tag{A10}$$

$$t_2 = \frac{v_y + \sqrt{v_y^2 + 3.244y_1}}{1.622} \tag{A11}$$

We now return to equation (A1). Substituting equations (A4) and (A5) in for x_1 and x_2, respectively, we arrive at equation (A12).

$$r = 0.5a_x t_1^2 + v_x t_2 \tag{A12}$$

We can now substitute equations (A9), (A10), (A7), and (A11) in for a_x, t_1, v_x, and t_2 respectively, arriving at equation (A13):

$$r = \left(0.5 \left(\frac{\frac{F\sqrt{2}}{2}}{m} \right) \left(\frac{I_{sp} \times 9.81 \times 1.021L}{F} \right)^2 + (a_x t_1) \frac{v_y + \sqrt{v_y^2 + 4 \times 0.5 \times 1.622y_1}}{1.622} \right) \tag{A13}$$

Our goal is to substitute until only the variables F, L, I_{sp}, and m remain. Showing all the substitutions is unnecessary, but it is easily verifiable that further substitutions using equations (A9) and (A10) for the a_x and t_1 respectively and equations (A6), (A8), and (A10) for v_y yields the messy equation (A14).

$$r = 0.5\frac{\frac{F\sqrt{2}}{2}}{m}\left(\frac{9.81I_{sp}\times 1.021L}{F}\right)^2 + \left(\frac{\frac{F\sqrt{2}}{2}}{m}\right)\left(\frac{9.81I_{sp}\times 1.021L}{F}\right)\frac{\left(\left(\frac{\frac{F\sqrt{2}}{2}}{m}-1.622\times m\right)\left(\frac{9.81I_{sp}\times 1.021L}{F}\right)\right)+\sqrt{\left(\left(\frac{\frac{F\sqrt{2}}{2}}{m}-1.622\times m\right)\left(\frac{9.81I_{sp}\times 1.021L}{F}\right)\right)^2+3.244\times 0.5\frac{\frac{F\sqrt{2}}{2}}{m}-1.622\times m\left(\frac{9.81I_{sp}\times 1.021L}{F}\right)^2}}{1.622} \quad (A14)$$

However, this equation, while correct, has a couple of issues. First, it is unsimplified. Second, equation (A14) outputs distance in meters, and we would like to look at outputs in kilometers. Both of these issues are fixed in equation (A15). We can see that equation (A15) is the same as equation (1).

$$r = \frac{\left(9.81I_{sp}\right)^2(1.021L)^2}{1000}\left(\frac{\sqrt{2}}{4mF} + \frac{\sqrt{2}}{3.244m}\left(\frac{\sqrt{2}+\sqrt{2-\frac{3.244\sqrt{2}m}{F}}}{2m} - \frac{1.622}{F}\right)\right) \quad (A15)$$

We verified this equation by putting all equations into Desmos and verifying equations (A15) and (A2) with implied substitutions are indeed equivalent.

References

[1] R. E. Yates, "Deployable Lunar Hopper (Hopper-TP)," National Aeronautics and Space Administration, Houston, Texas, 2026.

[2] K. E. Smith, A. Colaprete, R. Elphic, J. Captain, J. Quinn and K. Zacny, "The Volatiles Investigating Polar Exploration Rover Payload," in *Lunar and Planetary Science Conference*, The Woodlands, Texas, 2020.

[3] J. M. Schuler, J. D. Smith, A. J. Nick, B. C. Buckles, J. E. Dyas, V. V. Ortega, J. M. Cloud, A. G. Dokos, E. L. Zhang, J. J. Wang, M. A. Baron, T. J. Muller, C. J. Clark and M. W. Howe, "ISRU Pilot Excavator (IPEx) Technology Readiness Level 5 Design Overview," National Aeronautics and Space Administration Kennedy Space Center, Merritt Island, Florida, 2024.

[4] National Aeronautics and Space Administration Jet Propulsion Laboratory, "NASA Testing Advanced Capabilities for Moon, Mars Rovers," 18 June 2026. [Online]. Available: https://www.nasa.gov/solar-system/moon/nasa-testing-advanced-capabilities-for-moon-mars-rovers/.

[5] National Aeronautics and Space Administration, "MoonFall," [Online]. Available: https://www.jpl.nasa.gov/missions/moonfall/.

[6] C. Warner, "Lunar Living: NASA's Artemis Base Camp Concept," 28 October 2020. [Online]. Available: https://www.nasa.gov/blogs/artemis/2020/10/28/lunar-living-nasas-artemis-base-camp-concept/.

[7] P. D. Spudis, "History of Lunar Exploration," 27 September 2017. [Online]. Available: https://science.nasa.gov/solar-system/moon/history-of-lunar-exploration/.

[8] C.-H. Mattei, "Ranger 7," 2 November 2024. [Online]. Available: https://science.nasa.gov/mission/ranger-7/.

[9] National Aeronautics and Space Administration, "About LRO," 1 July 2025. [Online]. Available: https://science.nasa.gov/mission/lro/about/.

[10] J. Mehta, "The Moon, gateway for science and exploration," April 2024. [Online]. Available: https://www.planetary.org/worlds/the-moon.

[11] National Aeronautics and Space Administration, "Moon Exploration," 27 May 2026. [Online]. Available: https://science.nasa.gov/moon/exploration/.

[12] National Aeronautics and Space Administration, "Commercial Lunar Payload Services," 15 June 2023. [Online]. Available: https://www.nasa.gov/reference/commercial-lunar-payload-services/.

[13] The Planetary Society, "Every Mission to the Moon, Ever," 2026. [Online]. Available: https://www.planetary.org/space-missions/every-moon-mission.

[14] Y. Shi, X. Lin, M. Mohammadi and A. Huang, "Laser Powder Bed Fusion," 2022. [Online]. Available: https://www.sciencedirect.com/topics/materials-science/laser-powder-bed-fusion#definition.

[15] R. Hoover, "Part 1: Artificial Intelligence and NASA's First Robotic Lunar Rover," 1 December 2023. [Online]. Available: https://www.nasa.gov/blogs/missions/2023/12/01/part-1-artificial-intelligence-and-nasas-first-robotic-lunar-rover/.

[16] T. E. Cohen and D. S. Lees, "Exploration Ground Data Systems (xGDS) Overview," National Aeronautics and Space Administration Ames Research Center, Moffett Field, California, 2018.

[17] J. A. Collins, J. Michel and K. Araghi, "LUNAR WATER EXTRACTION via LUNAR AUGER DRYER ISRU (LADI)," National Aeronautics and Space Administration Johnson Space Center, Houston, Texas, 2023.

[18] M. Hamm, M. Grott, J. Knollenberg, N. Müller, M. S. Robinson, M. Atwell and T. Martin, "LRAD – A RADIOMETER FOR THE LUNAR SOUTH POLE HOPPER μNOVA," Lunar and Planetary Science Conference, The Woodlands, Texas, 2022.

[19] B. A. Campbell, B. R. Hawke and T. W. Thompson, "Long-wavelength Radar Studies of the Lunar Maria," National Aeronautics and Space Administration Jet Propulsion Laboratory, La Cañada Flintridge, California, 1995.

[20] Y.-Q. J. Wenzhe Fa, "Simulation of brightness temperature from lunar surface and inversion of regolith-layer thickness," *Journal of Geophysical Research: Planets,* vol. 112, no. E5, 2007.

[21] T. D. Martin, N. Agrawal, M. J. Atwell, D. B. J. Bussey, N. M. Estes, M. Grott, M. Hamm, J. Knollenberg, C. E. Miconi, T. Pacher, M. S. Robinson, E. S. Speyerer and R. V. Wagner, "μNOVA HOPPER: IN-SITU EXPLORATION OF CHALLENGING TERRAINS," in *Lunar and Planetary Science Conference*, The Woodlands, Texas, 2025.

[22] National Aeronautics and Space Administration, "VIPER: Rover and Instruments," 21 September 2023. [Online]. Available: https://science.nasa.gov/mission/viper/rover-and-instruments/.

[23] D. Andrews, B. Bluethmann, T. Fong, T. Colaprete, S. Jara, T. Luzod, D. Petri, J. Trimble and R. Vaughan, "VIPER Industry Day: Technical Breifing, Questions and Answers," National Aeronautics and Space Administration, Washington, D.C., 2025.

[24] National Aeronautics and Space Administration Goddard Flight Center, "3D Lidar for Autonomous Landing Site Selection," [Online]. Available: https://technology.nasa.gov/patent/GSC-TOPS-353.

[25] Ariane Group, "Monopropellant Hydrazine Thrusters," 2024. [Online]. Available: https://www.space-propulsion.com/spacecraft-propulsion/hydrazine-thrusters/index.html.

[26] J. Captain, B. A. Ayala, M. Hancock, D. Archer, A. McAdam, A. Jarnot, A. Gawronska, J. Kleinhenz and R. Carro, "PRIME-1: MSolo Overview and Results," National Aeronautics and Space Administration, Washington, D.C., 2026.

[27] Intuitive Machines, "IM-2 Press Kit," Intuitive Machines, Houston, Texas.

[28] K. Valentine, "NASA funds hopper to explore lunar polar craters," 21 July 2021. [Online]. Available: https://news.asu.edu/20210720-nasa-funds-hopper-explore-lunar-polar-craters.

[29] C. J. Clark, V. V. Ortega, J. D. Smith, J. M. Schuler, J. Lahl, A. J. Nick and J. E. Dyas, "Design & Testing of TRL5 IPEx Actuators," in *IEEE Aerospace Conference*, Big Sky, Montana, 2025.

[30] J.-G. Kang, J. Park, T.-G. Song, J.-H. Kim, S. Hong and H.-W. Park, "Agile perceptive multi-skill locomotion for quadrupedal robots in the wild," *Science Robotics,* vol. 11, no. 116, 2026.

[31] National Aeronautics and Space Administration, "Infrastructure Pilot Excavator," 17 July 2026. [Online]. Available: https://www.nasa.gov/infrastructure-pilot-excavator/.

[32] K. Tate, "NASA's Mighty Saturn V Moon Rocket Explained," Space.com, Huntsville, Alabama, 2012.

[33] E. Howell, "NASA's Mighty Saturn V Moon Rocket: 10 Surprising Facts," Space.com, Huntsville, Alabama, 2017.

[34] C. Iantaffi, C. L. A. Leung, G. Maddison, E. Bele, S. Hocine, R. Snell, A. Rack, M. Meisnar, T. Rohr, I. Todd and P. D. Lee, "Laser Additive Manufacturing of Lunar Regolith Simulant: new insights from in situ Synchrotron X-ray Imaging," Elsevier, Amsterdam, Netherlands, 2025.

[35] T. Wright, "How Things Work: Electromagnetic Catapults," January 2007. [Online]. Available: https://www.smithsonianmag.com/air-space-magazine/how-things-work-electromagnetic-catapults-14474260/.

[36] National Library of Medicine, "PRODUCTION, IMPORT, USE, AND DISPOSAL," *Toxicological Profile for Hydrazines,* vol. 4, 1997.

[37] National Aeronautics and Space Administration, "Moon Base," 5 August 2026. [Online]. Available: https://www.nasa.gov/moonbase/.

[38] J. Trimble, "VIPER Lunar Rover Agile Mission Systems," in *SpaceOps*, Dubai, United Arab Emirates, 2023.

[39] National Aeronautics and Space Administration, "Polar Resources Ice Mining Experiment 1 (PRIME-1)," 11 March 2025. [Online]. Available: https://www.nasa.gov/mission/polar-resources-ice-mining-experiment-1-prime-1/.

[40] European Space Agency, "3D-printed lunar base design," 2026. [Online]. Available: https://www.esa.int/ESA_Multimedia/Images/2013/01/3D-printed_lunar_base_design. ESA Standard License: https://www.esa.int/ESA_Multimedia/Terms_and_conditions_of_use_of_images_and_videos_available_on_the_esa_website

[41] National Aeronautics and Space Administration, "Building the Future: Space Station Crew 3-D Prints First Student-Designed Tool in Space," 15 June 2016. [Online]. Available: https://www.nasa.gov/missions/station/building-the-future-space-station-crew-3-d-prints-first-student-designed-tool-in-space/.